Energy Efficiency Dynamics and Climate Policy

Gregory Casey and Yang Gao

August 2024

Abstract

We study the effectiveness of climate change mitigation policies in reducing carbon emissions, focusing on the channel of economy-wide energy efficiency. Using U.S. data, we estimate impulse response functions (IRFs) that characterize how energy efficiency responds to energy price shocks. Standard climate-economy models cannot replicate the slow transition dynamics observed in the data. We build a tractable model that nests the existing literature and can closely replicate the empirical IRFs. The slow dynamics in our model imply that carbon taxes reduce emissions less than predicted by standard models and that clean energy subsidies reduce emissions more than predicted by standard models.

Keywords Climate Change, Climate Policy, Energy Efficiency

JEL Codes E24, O33, O44

Casey: Department of Economics, Williams College, gpc2@williams.edu. Gao: Department of Economics, University of California Santa Barbara, yang_gao@ucsb.edu. Casey gratefully acknowledges financial support from National Science Foundation Grant SES-2315408.

We thank Stefan Hinkelmann, Jason Jones, Peter Kruse-Andersen, Ken Kuttner, Peter Pedroni and seminar participants at SURED, AERE, AERE@EEA, AERE@MEA, Brown, and UC Santa Barbara for helpful feedback. All errors are our own.

1 Introduction

Many national governments are instituting policies meant to reduce carbon emissions. How effective will these *climate change mitigation* policies be at reducing carbon emissions? We address this question in a quantitative, dynamic climate-economy model with realistic transition dynamics. Transition dynamics are crucial to climate policy analysis for two reasons. First, climate change is a function of the stock of carbon in the atmosphere, rather than the flow of emissions. So, the environmental impact of a mitigation policy depends on how it affects emissions in the short-, medium- and long-run. Second, many climate policy goals are framed in terms of medium-run emissions. For example, the United States' Nationally Determined Contribution to the Paris Agreement focuses on targets for flow emissions in 2030.[1] Despite the importance of transition dynamics for climate policy analysis, existing climate-economy models are calibrated to static or steady state moments (e.g., Golosov et al., 2014; Hassler et al., 2016; Hassler and Krusell, 2018; Barrage and Nordhaus, 2023).[2] In other words, they are designed to correctly capture long-run outcomes and not designed to have realistic transition dynamics. A recent memo from the Biden Administration highlights the need for climate-economy models with better transition dynamics, because such models would allow for more evidenced-based policymaking.[3]

We focus on the dynamics of energy efficiency, an important determinant of carbon emissions (Raupach et al., 2007; Peters et al., 2017; Le Quéré et al., 2019). Put differently, we study substitution between energy and non-energy factors of production. Existing work finds that the short-run elasticity of substitution is near zero, but the long-run elasticity is around one (Atkeson and Kehoe, 1999; Hassler et al., 2021a). Climate economy models generally

[1] Indeed, the document is subtitled "Reducing Greenhouse Gases in the United States: A 2030 Emissions Target". See the entry for the United States at: http://tinyurl.com/57xn9fez.

[2] An exception is a literature that integrates climate change into business cycle analysis to look at the impacts of environmental policy over very short time horizons (e.g., Heutel, 2012; Annicchiarico and Di Dio, 2015; Känzig, 2023). As in the standard models, we examine impacts over longer time horizons in order to determine the full impacts of climate policy. Bilal and Rossi-Hansberg (2023) generate realistic transitions following climate impacts, like hurricanes and heat waves, rather than climate policy, in a long-run model. Relatedly, Klenow et al. (2023) study the long-run, dynamic impacts of temperature shocks. Metcalf and Stock (2023) study the effect of carbon taxes on macroeconomic outcomes and emissions, but do not match a model to data.

[3] The memo lists six areas for improvement in climate-economy models. Number 2, 'Account for transitional dynamics and frictions,' is the most relevant. Relative to existing work, the model developed in this paper also improves on Number 6, 'Include short- and intermediate-term timescales and greater spatial granularity', by considering a model with an annual time step and improves on Number 1, 'Include nonprice policies', by studying the impacts of clean energy subsidies in addition to a carbon price. See https://www.whitehouse.gov/wp-content/uploads/2023/12/Memo_Tools-for-Near-Term-Climate-Risk-Management.pdf.

assume that the elasticity is one in both the short and long run (e.g., Golosov et al., 2014; Hassler et al., 2016; Barrage, 2020; Cruz and Rossi-Hansberg, 2024). This causes standard models to overestimate the degree to which energy efficiency reacts to policy-induced changes in energy prices in the short and medium run (Casey, 2024).

To generate realistic dynamics in our model, we incorporate the insights of Hassler et al. (2021a) and the modeling framework of Leon-Ledesma and Satchi (2019) into a neoclassical production setting where final goods are produced with capital, labor, and energy. The result is a tractable setting in which the elasticity of substitution between energy and non-energy inputs can vary over time due to endogenous technology choice. We consider a model with two types of technology, both of which increase output. One technology augments energy and improves energy efficiency, and the other technology augments a capital-labor composite and decreases energy efficiency. Firms pay an adjustment cost when they alter their technology mix. The size of the adjustment costs determines how slowly energy efficiency responds to a change in energy prices.

We calibrate to the energy efficiency transition dynamics observed in the data. We use aggregate US data on energy use and energy prices from the Energy Information Administration (EIA) to estimate empirical impulse response functions (IRFs) that show how economy-wide energy efficiency responds to changes in the real price of energy. The IRFs describe the short- and medium-run transition dynamics. They suggest that energy efficiency responds slowly to changes in energy prices. We calibrate the adjustment costs and short-run substitution elasticity in the model so that it generates IRFs that are similar to those estimated in the data.[4] The calibrated model fits the data closely. We also show that the approach used in leading climate-economy models cannot replicate the patterns observed in the data, because it assumes that energy efficiency responds quickly to changes in energy prices.

To analyze the importance of slow transition dynamics, we use the model to study the effectiveness of climate change mitigation policies. We focus on comparing our results to the standard approach used in the existing literature. We examine carbon taxes, the most commonly discussed mitigation policy, and clean energy subsidies, a central climate tool in the Inflation Reduction Act (IRA).

Slow transition dynamics significantly hinder the ability of carbon taxes to reduce cumulative carbon emissions. Carbon taxes increase the price of energy and induce substitution away from energy and toward non-energy inputs. In other words, they increase energy

[4]This process of IRF matching is a common method of calibrating parameters in the business-cycle literature. As far as we are aware, it has not been previously used to study the impacts of climate policy.

efficiency. In our model and the data, this process happens slowly, as firms adjust their technology choices to respond to changes in tax-inclusive energy prices. In standard models, however, the adjustment process happens immediately. Our model predicts that a 50 percent value-added carbon tax reduces cumulative carbon emissions by 19 percent over the next decade, relative to a no-policy scenario. In the standard model, by contrast, the same tax reduces emissions by 35 percent. By this metric, accounting for the slow transition dynamics in the data reduces the estimated effectiveness of carbon taxes by half.

Conversely, slow transition dynamics significantly bolster the ability of clean energy subsidies to reduce cumulative carbon emissions. Unlike carbon taxes, clean energy subsidies decrease the price of energy, inducing substitution towards energy inputs and decreasing energy efficiency (Holland et al., 2009; Newell et al., 2019). As a result, these policies are more effective when energy efficiency dynamics are slow. Our model predicts that a 20 percent subsidy for clean energy reduces cumulative carbon emissions by 4 percent over the next decade, relative to laissez-faire. In the standard model, by contrast, the same path of subsidies increases emissions by 1 percent.

Related Literature. Starting with the DICE model (Nordhaus, 1993), many studies have investigated climate policy using growth models (e.g., Golosov et al., 2014; Hassler et al., 2021b; Barrage and Nordhaus, 2023; Cruz and Rossi-Hansberg, 2024). When energy efficiency is included in these models, it is generally done with a Cobb-Douglas aggregate production function, implying that the short- and long-run elasticities of substitution are both equal to one. This implies that energy efficiency reacts quickly to changes in energy prices. We build on this literature by constructing a model that matches the empirical dynamics of energy efficiency and showing that these dynamics have significant consequences for the effectiveness of mitigation policies.

There is also long literature documenting empirical facts about energy use (e.g., Van der Werf, 2008; Koetse et al., 2008), including the fact that the elasticity of substitution differs in the short and long run (e.g., Pindyck, 1979; Hassler et al., 2021a). There is also a long literature presenting models that explain the difference between the short- and long-run elasticities. Older models relied on putty-putty or putty-clay models with adjustment costs and many types of capital (e.g., Pindyck and Rotemberg, 1983; Atkeson and Kehoe, 1999), while newer models stress directed technical change in more aggregated settings (e.g., André and Smulders, 2014; Hassler et al., 2021a). We contribute to this literature by estimating the full transition dynamics that occur as an economy moves from the short run to the long

run and by demonstrating the importance of these slow dynamics for the effectiveness of climate change mitigation policies.

Our work also contributes to a small but growing literature on transition dynamics and climate policy. The most closely related paper is Casey (2024), which uses a model of directed technical change to study the role of energy efficiency transition dynamics in determining the effectiveness of carbon taxes. The model is calibrated to steady state moments only. It utilizes a short-run elasticity of zero and does not report a long-run elasticity, which cannot be found analytically. As noted above, our work builds on insights from Hassler et al. (2021a). In their empirical application, they estimate an endogenous growth model with annual data, but do not match transition dynamics. Building on these works, Hinkelmann (2023) considers a richer model with several margins of adjustment and similarly shows that transition dynamics matter for the design of carbon taxes that can implement medium-run climate policy goals in the United States. Like us, he utilizes the production structure of Leon-Ledesma and Satchi (2019), but he does not match the transition dynamics to data.[5,6] Airaudo et al. (2023) take a somewhat different approach and embed the framework of Hassler et al. (2021a) in a open-economy business cycle model to study the impact of climate policy on both economic and environmental outcomes. Campiglio et al. (2022) study optimal climate policy in a model with capital adjustment costs. They calibrate their model to the outcomes of granular energy models, rather than directly to the transition dynamics observed in aggregate data. Like us, they find that transition dynamics play an important role in climate policy. Our work complements these earlier studies in two ways. First, and most importantly, we match our model to the transition dynamics observed in data. Second, we stress the differential effect of energy efficiency dynamics on carbon taxes and clean energy subsidies, the latter of which is central to recent climate legislation in the United States.

2 Model

2.1 Model Specification

Time is discrete and indexed by t. Each period corresponds to one year. All production is perfectly competitive. Our model is focused on aggregate energy efficiency, i.e., substitution

[5] See also Hinkelmann and Farajpour (2021), who confirm the importance of distinguishing between short- and long-run elasticities, but do not include transition dynamics.

[6] Hinkelmann (2024) uses related tools to study substitution between electricity and fossil fuels.

between energy and non-energy inputs to production. The representative final good producer has access to a CES production technology:

$$\tilde{Y}_t = \left((A_{N,t} N_t)^{\frac{\epsilon-1}{\epsilon}} + (A_{E,t} E_t)^{\frac{\epsilon-1}{\epsilon}} \right)^{\frac{\epsilon}{\epsilon-1}}, \tag{1}$$

where $\tilde{Y}_t$ is gross output, N_t is non-energy inputs in productions (capital and labor), E_t is energy, and $\epsilon \in (0, \infty)$. The variable $A_{N,t}$ is non-energy-augmenting technology, and $A_{E,t}$ is energy-augmenting technology, which is closely related to energy efficiency. The final good producer chooses a sequence of inputs, $\{K_t, L, E_t\}_{t=0}^{\infty}$, and a sequence of technologies, $\{A_{N,t}, A_{E,t}\}_{t=0}^{\infty}$, to maximize the expected present discounted value of future profits. The price of the final good is normalized to one, and we use $p_{N,t}$ to denote the price of the non-energy composite.

The representative producer can choose the two technology terms from a menu

$$x_t = (1-\eta) \ln A_{N,t} + \eta \ln A_{E,t}, \tag{2}$$

where x_t captures the overall level of technology. We also define $X_t := e^{x_t}$. As shown below, this will be a natural measure of the overall level of technology in the economy. The growth rate of X_t, $g_{X,t}$, follows a stochastic $AR(1)$ process

$$g_{X,t} = (1-\rho_X)\mu_X + \rho_X g_{X,t-1} + \omega_{X,t}, \tag{3}$$

where $\omega_{X,t} \sim \mathcal{N}(0, \Sigma_X^2)$ is an $i.i.d.$ shock and μ_X is a long-run drift parameter. The producer chooses current-period technologies prior to the realization of $\omega_{X,t}$.

Let $\theta_t \equiv A_{E,t}/A_{N,t}$ be the technology ratio. When firms adjust θ_t, they lose a fraction of total output due to a quadratic adjustment costs

$$\Phi\left(\frac{\theta_t}{\theta_{t-1}}\right) = \frac{\phi}{2}\left(\frac{\theta_t}{\theta_{t-1}} - 1\right)^2. \tag{4}$$

Given the convex adjustment costs, firms adjust θ_t slowly over time in response to a change in relative input prices. Parameter ϕ determines how quickly this adjustment occurs.

Combining production function (1) and the technology menu (2), output can be written as

$$\tilde{Y}_t = X_t \left(\left(\theta_t^{-\eta} N_t\right)^{\frac{\epsilon-1}{\epsilon}} + \left(\theta_t^{1-\eta} E_t\right)^{\frac{\epsilon-1}{\epsilon}} \right)^{\frac{\epsilon}{\epsilon-1}}. \tag{5}$$

The overall level of technology, X_t, is exogenous and the direction of technology, θ_t, is endogenous.

An intermediate producer combines capital and labor into the non-energy input bundle using a Cobb-Douglas technology:

$$N_t = K_t^{\alpha} L^{1-\alpha}. \tag{6}$$

We assume that the size of the labor force is constant. For prices, w_t denotes the wage rate, ρ_t denotes the rental rate on capital, and $\alpha \in (0, 1)$.

Energy is extracted from the environment using the final good and a linear production technology, implying that $p_{E,t}$ is equal to the real extraction cost. The energy price growth follows a stochastic $AR(1)$ process

$$g_{p_{E,t}} = (1 - \rho_{p_E})\mu_{p_E} + \rho_{p_E} g_{p_{E,t-1}} + \omega_{p_{E,t}}, \tag{7}$$

where $\omega_{p_{E,t}} \sim \mathcal{N}(0, \Sigma_{p_E}^2)$ is an $i.i.d.$ shock to the growth rate of energy prices in each period and μ_{p_E} is the long-run drift parameter. Again, firms choose current-period technology levels prior to the realization of the shock.

Final output (Y_t) is gross output minus energy expenditures and adjustment costs:

$$Y_t = \left(1 - \frac{\phi}{2}\left(\frac{\theta_t}{\theta_{t-1}} - 1\right)^2\right) \times \tilde{Y}_t - p_{E,t} E_t. \tag{8}$$

This is the measure of gross domestic product (GDP) in our model.

A representative household chooses a sequence of consumption (C_t) and investment (I_t) to maximize expected lifetime utility

$$U := \mathbb{E}_0 \left(\sum_{t=0}^{\infty} \beta^t \ln(C_t) \right), \tag{9}$$

taking all prices and technology levels as given. Here, $\beta \in (0, 1)$ is the discount factor. The budget constraint for the representative household is

$$C_t + I_t = w_t L + \rho_t K_t = Y_t. \tag{10}$$

Capital evolves according to

$$K_{t+1} = I_t + (1 - \delta) K_t, \tag{11}$$

where $\delta \in (0, 1)$ is the depreciation rate.

We now have all of the components necessary to define a competitive equilibrium.[7]

Definition 1. *A* competitive equilibrium *is a sequence of prices, quantities, and technologies such that (1) firms maximize profits, (2) all market clearing conditions hold, and (3) individuals maximize lifetime utility.*

We have not specified the costs of climate change in either the production or utility functions. Our focus is on the determinants, rather than the consequences, of carbon emissions. Since relatively little is known about the magnitude of climate impacts (Auffhammer, 2018), we prefer to quantify our results in terms of the quantity of dirty energy use, rather than attempting to translate energy use into changes in temperature, utility or productivity. The fact that climate change doesn't affect economic dynamics is equivalent to a setting where the costs of climate change enter the utility function in an additive form (see, e.g., Barrage, 2020). Recent work on the social cost of climate change suggests that much of the damages come from the non-market impacts of climate (e.g., Rennert et al., 2022b).

2.2 The Elasticity of Substitution (EoS)

2.2.1 Short- versus Long-Run EoS

The key idea behind this production structure is that, following a change in energy prices, the economy behaves differently in the short and long run. In the very short run, technology is fixed and the producer can only respond to energy prices by substituting non-energy inputs for energy inputs using the CES function (1). At longer time horizons, the producer can also change technology terms, which makes production more flexible and leads to more substitution in response to change in relative prices.

To further explore this intuition in terms of the elasticity of substitution between energy and non-energy inputs, we will now briefly discuss the theoretical results from Leon-Ledesma and Satchi (2019), which is the basis for our model.

They define the *short-run elasticity of substitution* as

$$\sigma_{SR} := -\frac{d \ln(\frac{E_t}{N_t})}{d \ln(\frac{p_{E,t}}{p_{N,t}})}\bigg|_{\theta_t \text{ fixed}}. \tag{12}$$

When climate policy or supply shocks increase the relative price of energy, σ_{SR} describes the immediate reaction of firms. The *long-run elasticity of substitution* (σ_{LR}) is the elasticity of

[7] Appendix Section A presents the full set of equilibrium equations for the model.

substitution when θ_t has fully adjusted to its profit-maximizing level:

$$\sigma_{LR} := -\frac{d\ln(\frac{E_t}{N_t})}{d\ln(\frac{p_{E,t}}{p_{N,t}})}\bigg|_{\frac{\partial \Pi_t}{\partial \theta_t}=0}, \tag{13}$$

where Π_t is profits earned by the final good producer in period t. When climate policy or supply shocks increase the relative price of energy, σ_{LR} describes the long-run reaction of firms.[8]

Proposition 1. *Consider a production setting given by the production function (1) and the technology menu (2). In this case, $\sigma_{SR} = \epsilon$ and $\sigma_{LR} = 1$.*

Proof. This is a special case of Proposition 3 in Leon-Ledesma and Satchi (2019). We provide a simple proof in Appendix Section A.2. □

2.2.2 EoS and the Energy Expenditure Share

In our empirical application, we estimate the impact of energy price shocks on the energy expenditure share of output. To see how these objects are related, let σ be the EoS for some time horizon. Taking the definition of the EoS and integrating,

$$\ln \frac{E_t}{N_t} = \text{constant} + \sigma \ln \frac{p_{N,t}}{p_{E,t}}. \tag{14}$$

Subtracting $\ln \frac{p_{N,t}}{p_{E,t}}$ from both sides gives

$$\ln \frac{p_{E,t}E_t}{p_{N,t}N_t} = \text{constant} + (\sigma - 1) \ln \frac{p_{N,t}}{p_{E,t}}. \tag{15}$$

Now, we restrict attention to outcomes when there are no adjustment costs. This captures the long-run elasticity (after all adjustment costs are paid) and the short-run elasticity (before any adjustment costs are paid). With perfect competition, total revenue is equal to payments to energy producers plus payment to non-energy factors of production. So, we can re-write our expression as

$$\ln \frac{s_{E,t}}{1 - s_{E,t}} = \text{constant} + (\sigma - 1) \ln \frac{p_{N,t}}{p_{E,t}}, \tag{16}$$

[8] The definition of σ_{LR} from Leon-Ledesma and Satchi (2019) refers to a firm that only maximizes single-period profits. In our empirical applications, we study a firm that maximizes the present discounted value of profits in an environment where the energy price is constantly changing.

where

$$s_{E,t} := \frac{p_{E,t}E_t}{Y_t + p_{E,t}E_t}, \tag{17}$$

is the *energy expenditure share of output*. We use this measure of the energy expenditure share for two reasons. The first is to be consistent with the data. It would be natural to measure to energy expenditure share in terms of gross output, but we would need a measure of adjustment cost expenditure to calculate gross output in a way that is consistent with our model. Unfortunately, there is not straightforward way to do this. The second reason that we choose this measure is to facilitate comparisons with the existing literature. As discussed below, the existing literature makes stark predictions about how this measure of the energy expenditure share responds to a price shock, making it easy to compare the predictions of the existing literature to our model and the data.

In our empirical application, we study how exogenous shocks to $p_{E,t}$ affect the dynamics of $s_{E,t}$, and then match the dynamics to our model. Equation (16) shows how these objects are related, though we will not be able to estimate it directly. For this reason, our estimation procedure is in the spirit of indirect inference (Smith, 2008).[9]

2.3 Comparison to Existing Literature

In the macro climate economy literature, it is standard to use a Cobb-Douglas (CD) production function for final output,

$$Y_t = K_t^{\alpha} E_t^{\nu} \left(A_t L\right)^{1-\alpha-\nu}.$$

This production function assumes $\sigma_{\text{SR}} = \sigma_{\text{LR}} = 1$. Thus, it has the same long-run predictions as our model, but different short- and medium-run predictions. Indeed, this production function is a special case of our model with $\epsilon = 1$ and $\phi = 0$. The CD production function implies that the energy expenditure share is $s_{E,t}^{\text{CD}} = \nu \ \forall t$. Thus, we can easily test the predictions of this model against the data by examining how the expenditure share responds to changes in the real energy price. The data presented in Figure 1 suggest that this production function will not be a good match for the data at short time horizons.

[9]Since the price of output is normalized to one, the endogenous object $p_{N,t}$ is a function of only the price of energy and the production function parameters. Since we are estimating the production function parameters, we do not have a closed form equation that we can take directly to the data. But, we are still in a scenario where we are examining how one endogenous variable, $s_{E,t}$, responds to shocks in one exogenous variable, $p_{E,t}$.

3 Matching the Model to Data

In this section, we discuss the empirical IRFs and how we use them to calibrate the model. Existing climate-economy models are often calibrated to long-run averages, like the average energy share of expenditure. We instead want to calibrate our model to data patterns that capture transition dynamics as well as long-run averages.

3.1 Energy Data

Our energy data come from the State Energy Data System (SEDS) produced by the U.S. Energy Information Administration (EIA). Given that we are interested in macro elasticities, we focus on aggregate data for the United States. Appendix Section B provides further description of the data. The data include quantities for different types of primary energy (e.g., coal, oil, renewables) and final energy (e.g., electricity, gasoline). The data also include prices for most types of primary and final energy, but do not include prices for renewable sources of primary energy.

Our analysis uses two empirical objects, the energy expenditure share and the real price of final energy. As in the model, the energy expenditure share is measured as energy expenditure divided by the sum of final output (GDP) and energy expenditure. Our measure of the energy price is the BTU-weighted average across energy sources. Hassler et al. (2021a) propose a method of calculating aggregate prices that weights the quantities of different energy types by their average prices. In Appendix Section B.3, we show that this has virtually no effect on our price series. To convert nominal to real prices, we use the GDP deflator.

Figure 1 plots the two empirical objects. Panel (a) focuses on long-run trends. The real price of final energy has been increasing over this period, while the expenditure share has been been declining. Together, these two observations suggest an EoS between energy and non-energy inputs that is greater than one. Given the relatively short time period, it is hard to rule out the hypothesis that there is no trend in the share, which would suggest a long-run EoS of one. This is consistent with the econometric literature that distinguishes between short- and long-run elasticities and finds long-run elasticities at or above one (Griffin and Gregory, 1976; Pindyck, 1979; Koetse et al., 2008). The macro climate literature has interpreted the evidence as suggesting that a unitary elasticty, i.e Cobb-Douglas production, is a good fit for data (e.g., Golosov et al., 2014; Barrage, 2020; Hassler et al., 2021b). Since our goal is to demonstrate the importance of transition dynamics in climate-economy models, we follow the existing literature and focus on the case of a unitary long-run elasticity throughout

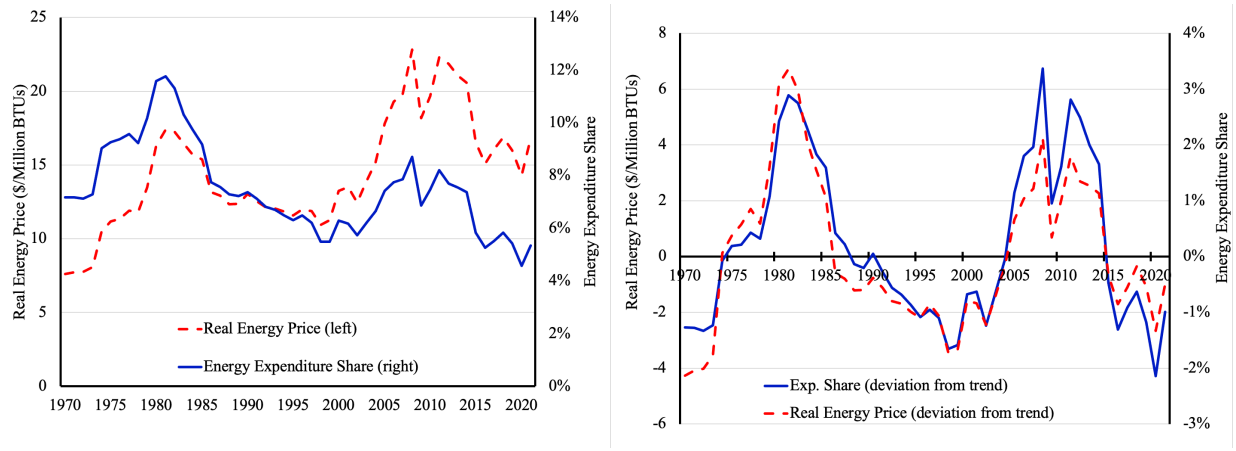

(a) Trends (b) Deviations

Figure 1: Final Energy Price and Expenditure Share

Note: Panel (a) shows the average real price of final energy ($2012/million BTU) and the energy expenditure share (% of GDP). Panel (b) shows the deviation of the real price from its deterministic exponential trend and the deviation of the energy expenditure share from its average value.

the paper. In other words, we assume that any trend in the expenditure share is unrelated to changes in the relative price of energy and non-energy inputs.

To highlight short- and medium-run fluctuations, panel (b) plots the deviations of real energy price and the expenditure share from their deterministic exponential trends. The two series move together closely, indicating that the short-run EoS is well below one. Again, this is consistent with the econometric literature, which finds short-run elasticities that are close to zero when looking at very short time horizons (e.g., Berndt and Wood, 1975; Hassler et al., 2021a).

3.2 Empirical Methodology

We use the annual data described in the previous section to estimate the impulse response function (IRF) of the energy expenditure share to a permanent change in the level of energy prices. To do so, we use a structural vector autoregression (SVAR). Our SVAR consists of the following two equations:

$$\Delta \ln (p_{E,t}) = \text{cons}_1 + a \cdot \Delta \ln (p_{E,t-1}) + u_1 \tag{18}$$

$$s_{E,t} = \text{cons}_2 + b \cdot \Delta \ln (p_{E,t-1}) + c \cdot s_{E,t-1} + u_2. \tag{19}$$

To identify shocks, we make the assumption that $u_1 = \epsilon_1$ and $u_2 = d\epsilon_1 + \epsilon_2$, where ϵ_1 and ϵ_2 are orthogonal structural shocks. Following the model, this specification assumes that energy prices evolve exogenously. In other words, it assumes that annual variation in energy prices is driven by supply shocks, which are captured by ϵ_1. Our IRFs focus on the dynamics following a one standard deviation shock to ϵ_1, which we refer to as an 'energy price shock'.

We use the de-trended energy expenditure share in our main specification, following Blanchard and Quah (1989). Thus, our analysis assumes that any trend in $s_{E,t}$ is unrelated to changes in the price of energy, as assumption that is consistent with the unitary elasticity of substitution used in the existing literature (Golosov et al., 2014). Appendix Section C.1 shows that the results are quantitatively and qualitatively similar if we do not de-trend the data.[10]

Our baseline VAR specification uses only one lag of the dependent variables. Appendix Section C.2 demonstrates that the empirical IRFs are quantitatively and qualitatively similar with three and five lags in equation (19). We also examined a number of lag selection criteria, all of which suggest that the optimal numbers of lags is one.[11]

3.3 External Model Parameters

We set a number of parameters exogenously. We set $\beta = 0.985$ and $\delta = 0.10$, which are standard values for annual models. We choose $\eta = 0.075$ to match the average energy expenditure share of output, which is approximately 7.5% in the EIA data.[12] We take the remaining parameter values to match the standard facts as reported in Jones (2016). The labor share of expenditure is $(1-\eta)(1-\alpha)$, which we set to 65%. This yields $\alpha = 0.30$. We normalize the labor force to one in all periods. Table 1 reports the values of all calibrated parameters.

[10] Appendix B.2 shows the time paths of $\Delta \ln(p_{E,t})$ and de-trended $s_{E,t}$.

[11] In particular, we used FPE, AIC, BIC, and HQIC. We ran the tests examining changes in lags for both VAR equations and when imposing the energy price growth follows an AR(1) process. Results of these tests are reported in Appendix Section C.2.

[12] In the model, η is not exactly equal to the energy share of output and the difference between the two is due to adjustment costs. In our calibrated model, the adjustment costs are a small fraction of output. So, we choose to pursue this external calibration of η, because it maintains transparency and computational simplicity. Alternatively, we could be to calibrate η jointly with θ and ϵ.

3.4 Calibration

3.4.1 Stochastic Processes for X_t and $p_{E,t}$

The parameters driving the law of motion of TFP (X_t) and energy prices ($p_{E,t}$) are calibrated from data. Equation (3) is estimated with total factor productivity (TFP) data covering 1970–2019.[13] which yields $\mu_X = 0.6\%$, $\rho_X = 0.07$ and $\Sigma_X = 0.01$. Similarly, we estimate equation (7) using energy price data from EIA. This yields a drift coefficient $\mu_{p_E} = 1.6\%$, a persistence parameter $\rho_{p_E} = 0.16$, and a standard deviation of the shocks, $\Sigma_{p_E} = 0.09$.

3.4.2 IRF Matching Methodology

We choose the remaining two parameters, ϕ and ϵ, so that the IRF generated by the model matches the IRF from the structural VAR. In the model, we study the IRF following a one standard deviation shock to $\omega_{p_{E,t}}$, the exogenous component of the energy price. This allows us to consider the exact same path of energy prices in the data and model. Then, we focus on choosing the remaining parameters to make the paths of the energy expenditure share as similar as possible.

To calibrate these parameters, we simulate IRFs from the model for a two-dimensional grid of potential values and compute the quadratic distance between empirical and model generated IRFs over a 40-year period. The weight assigned to each period in the quadratic distance corresponds to the inverse of the empirical estimate of IRF variances. We choose the pair (ϵ, ϕ) that minimizes this loss function. In practice, ϵ is primarily identified by the initial jump in $s_{E,t}$, and ϕ is primarily identified by the speed of the transition path.

3.4.3 Results

We study a positive and temporary shock to the growth rate of energy prices, which corresponds to a permanent change in the level of energy prices. We are interested in this type of shock, because we will use the model to study climate policies that permanently change the price of energy.

Our empirical results are presented in Figure 2.[14] In all panels, the horizontal axis shows years since the initial shock, and the vertical axis shows deviations from the initial steady state. Panels (a) and (b) show the shock to energy prices that will be used for the analysis.

[13] The data were originally obtained from the Federal Reserve Economic Database (FRED). Further details are provided in Appendix Section B.1.

[14] The estimated coefficients are: $a = 0.1591(0.1432)$, $b = 0.0088(0.0100)$, and $c = 0.9644(0.0165)$ (standard errors in parentheses).

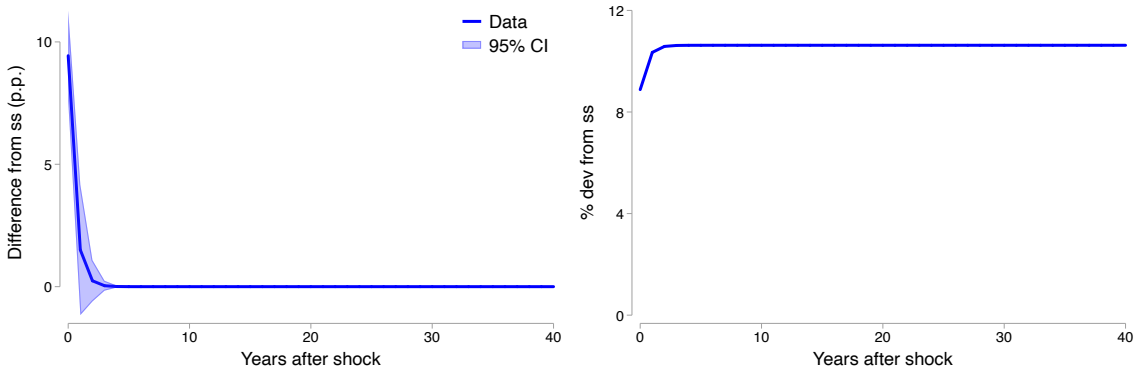

(a) Growth in Energy Prices

(b) Level of Energy Prices

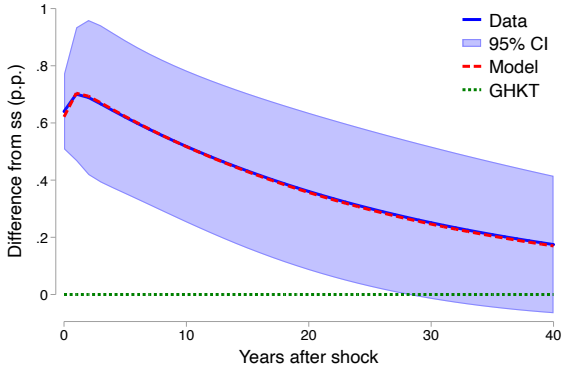

(c) Energy Share

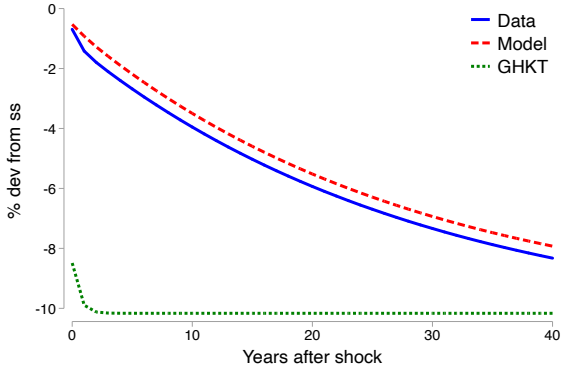

(d) Energy Intensity

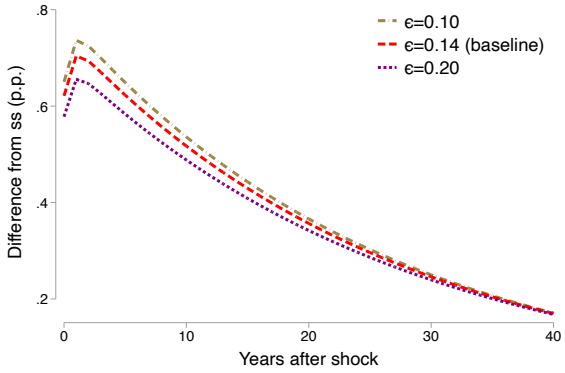

(e) Energy Share - ϵ Identification

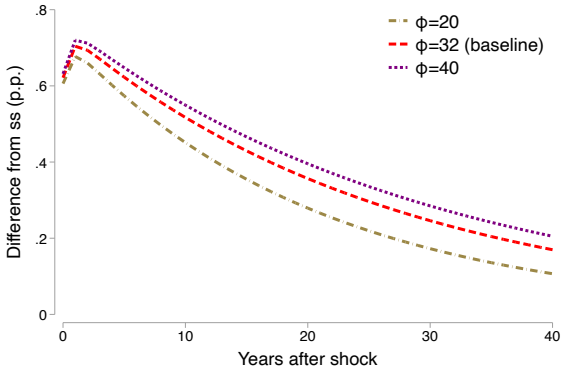

(f) Energy Share - ϕ Identification

Figure 2: Empirical Results and IRF Matching

Note: Panels (a) and (b) show the path of energy prices following a one standard deviation shock to the growth rate of energy prices. This path of energy prices is used in all subsequent analyses. Panel (c) shows the path of the energy expenditure share of output in the data (solid blue line), our calibrated model (dashed red line), and the special case of Golosov et al. (2014) (dotted green line). Panel (d) shows the implications for the energy intensity of output. Panels (e) and (f) illustrate how the impulse response functions (IRFs) identify the model parameters.

Panel (a) shows the dynamics of the energy price growth rate, which is estimated from the data. The blue line is the point estimate, and the bands are 95% confidence intervals. Panel (b) translates the changes in growth rates to changes in the level of energy prices. Energy prices reach their new level after 7 years.

We study the impact of this shock to energy prices in the data, our model, and older models from the literature. To represent the older literature, we focus on the influential model of Golosov et al. (2014) (henceforth, GHKT). They consider the case where $\sigma_{SR} = \sigma_{LR} = 1$. This specification is common in the literature (e.g., Nordhaus and Boyer, 2000; Hassler et al., 2016; Hassler and Krusell, 2018; Barrage, 2020; Cruz and Rossi-Hansberg, 2024) and is a special case of our model with $\phi = 0$ and $\epsilon = 1$.

Our main findings are shown in panel (c), which plots the response of the energy expenditure share to the energy price shock. The solid blue line is the IRF estimated from data, the dashed red line is our model with the parameters that best match the data, and the dotted green line is the GHKT special case. The empirical results line up closely with the findings and interpretations in the existing literature. In the period of the shock, a 9% increase in energy prices leads to a 0.64 percentage point (approximately 9%) jump in the expenditure share. As shown in equation (16), this result implies that the short-run EoS between energy and non-energy inputs is very close to zero, which is consistent with earlier work (e.g., Hassler et al., 2021a). The methodology imposes that the expenditure share eventually returns to the original level. In other words, it imposes that the long-run elasticity is equal to one. Relative to earlier work, a key benefit of our methodology is that we can estimate the full transition path following an energy price shock. The transition is quite slow, and the energy expenditure share has only returned halfway back to its original level 24 years after the shock.

Our calibrated model matches the data closely. This is unsurprising given that the model was constructed to be able to match both the short- and long-run EoS and to include a free parameter, ϕ, that governs the speed of the transition. Our calibration yields $\epsilon = 0.14$ ($= \sigma_{SR}$) and $\phi = 32$. In contrast, the GHKT specification is clearly at odds with the data. It imposes a short-run EoS of one, which implies that the energy expenditure share is unchanged following the energy price shock. The climate literature, including GHKT, is aware that the short-run EoS is a poor match for the data, but they argue that it accurately captures medium- and long-run dynamics (see also, Hassler et al., 2016, 2021b; Hassler and Krusell, 2018; Barrage, 2020). Our empirical results cast doubt on this assertion. The data and the GHKT approach predict very different energy expenditure shares over several decades.

Panel (d) demonstrates the implications of our findings. Panel (d) shows the path of the energy intensity – defined as $s_{E,t}/p_{E,t}$ – following the energy price shock. The curves are derived by dividing the path of $s_{E,t}$ from panel (c) by the path of $p_{E,t}$ from panel (b). This object is important for climate policy, because carbon taxes increase the price of energy and induce substitution towards non-energy inputs, reducing the energy intensity of output (i.e., increasing economy-wide energy efficiency). Both the data and our model suggest that this process happens slowly. There is essentially no increase in energy efficiency immediately following the shock, and the economy is still far from the new steady state after 30 years. In contrast, the GHKT model predicts that the adjustment is instantaneous. While the two models predict similar long-run outcomes, they have very different implications for short- and medium-run outcomes.[15]

Finally, panels (e) and (f) illustrate how the IRFs identify the model parameters. Panel (e) shows the effect of changing ϵ, holding ϕ fixed. In the period of the shock, the technology terms ($A_{N,t}$ and $A_{E,t}$) are fixed, and the EoS is given by $\sigma_{\text{SR}} = \epsilon$. Thus, ϵ plays a primary role in determining the size of the initial jump. Panel (f) shows the impact of changing ϕ, holding ϵ fixed. As discussed above, ϕ does not affect the short- or long-run EoS. But, higher values of ϕ imply that it is more costly to change the technology ratio, which in turn leads to slower transition dynamics. So, ϕ is largely determined by the speed of the transition.

4 Policy Analyses

We now turn to investigating the role that energy efficiency dynamics play in determining the effectiveness of climate change mitigation policies. In order to study the full non-linear impacts of policy, we abstract from uncertainty and use a deterministic version of the model. Our primary goal is to compare our calibrated model to the GHKT special case. We focus on outcomes over the next eighty years.

4.1 Set-up for Policy Analysis

To study the impact of climate policy on energy efficiency, we need to model how policies that affect clean and dirty energy impact the price of final energy. To accomplish this goal, Section 4.1.1 extends the model to include substitution between clean and dirty energy. Section 4.1.2 describes how the new parameters are calibrated.

[15] We calibrate the two models with the same parameter η. Since there are no adjustment costs in the GHKT special case, the energy share of expenditure differs slightly.

Table 1: Model Parameters

Parameter	Value	Description	Source
δ	0.10	Depreciation	Standard
β	0.985	Discount factor	Standard
η	0.075	Energy share of income	EIA
α	0.30	Capital share of income	Jones (2016)
μ_{p_E}	1.6%	Energy price drift	Calibrated
ρ_{p_E}	0.16	Energy price persistence	Calibrated
Σ_{p_E}	0.09	Energy price stan. dev.	Calibrated
μ_X	0.6%	TFP drift	Calibrated
ρ_X	0.07	TFP persistence	Calibrated
Σ_X	0.01	TFP stan. dev.	Calibrated
ϵ	0.14	Short-run EoS	IRF Matching
ϕ	32	Adjustment costs	IRF Matching
γ	0.74	Dirty energy share	EIA
g_{p_d}	1.9%	Dirty price growth	Calibrated
g_{p_c}	0.7%	Clean price growth	Calibrated
$p_{d,0}/p_{c,0}$	0.40	Relative energy price	Calibrated

4.1.1 Substitution between Clean and Dirty Primary Energy

We assume that the production function for final energy is given by

$$E_t = E_{d,t}^{\gamma} E_{c,t}^{1-\gamma}, \tag{20}$$

where E_d is the quantity of dirty energy and E_c is the quantity of clean energy. GHKT set the EoS between energy sources equal to 0.95, and we set it equal to one for computational convenience. We consider this simplified model, rather than allowing the elasticity to vary over time, because our focus is on the role of energy efficiency dynamics.

There is perfect competition in final energy production, and therefore the price of energy is

$$p_{E,t} = \tilde{\gamma}(1-\tau_{c,t})^{1-\gamma} p_{c,t}^{1-\gamma} (1+\tau_{d,t})^{\gamma} p_{d,t}^{\gamma}, \tag{21}$$

where $p_{c,t}$ is the cost of extracting clean energy from the environment, $p_{d,t}$ is the cost of extracting dirty energy from the environment, $\tau_{c,t} \geq 0$ is a subsidy for clean energy, $\tau_{d,t} \geq 0$ is a tax on dirty energy, and $\tilde{\gamma} = \gamma^{-\gamma}(1-\gamma)^{\gamma-1}$ is a constant. Extraction costs grow at

constant exogenous rates, g_{p_c} and g_{p_d}.[16] Equation (21) shows the key difference between carbon taxes and clean energy subsidies. Carbon taxes raise the price of final energy and promote energy efficiency, while clean energy subsidies decrease the price of final energy and discourage energy efficiency. Unlike the existing literature, our model accounts for the slow transition dynamics of energy efficiency. Adding slow energy efficiency dynamics to the model decreases the ability of carbon taxes to reduce emissions in the short- and medium-run, but increases the ability of clean energy subsidies to reduce emissions in the short- and medium-run.[17]

4.1.2 Calibration of Additional Parameters

With perfect competition, γ is equal to the ratio of expenditure on dirty sources of primary energy and all expenditure on final energy. In the data, the ratio is approximately 74% on average and does not appear to trend over time (see Casey and Gao, 2023, for further examination of this empirical observation). The EIA does not report the price of clean primary energy over this period. Production function (20) implies that

$$\frac{p_{d,t}}{p_{c,t}} = \frac{\gamma}{1-\gamma}\frac{E_{c,t}}{E_{d,t}}. \tag{23}$$

In 2019, the first year of our analysis, the ratio of clean and dirty primary energy, measured in BTUs, is equal to 0.14. Together with our estimate of γ, this implies that $\frac{p_{d,0}}{p_{c,0}} = 0.40$. To set units, we normalize the initial price of clean energy to one, $p_{c,0} = 1$.

We use a similar approach to pin down the growth rates of the energy prices. The ratio of clean to dirty energy grows at an average of 1.2%/year in our data. From (23), this implies that the relative price of clean energy decreases by 1.2%/year. Also, (21) implies that, in the absence of climate policy, the growth rate of the price of final energy is $g_{p_E} = (1+g_{p_c})^{1-\gamma}(1+g_{p_d})^{\gamma}-1$. This is equal to 1.6% in the data. Together, these two relationships give $g_{p_d} = 1.9\%$ and $g_{p_c} = 0.7\%$.

[16] With this specification for clean and dirty energy, final output becomes

$$Y_t = \left(1 - \frac{\phi}{2}\left(\frac{\theta_t}{\theta_{t-1}} - 1\right)^2\right) \times \tilde{Y}_t - p_{c,t}E_{c,t} - p_{d,t}E_{d,t}. \tag{22}$$

[17] Appendix Section A.5 provides the equilibrium equations for the extended model with clean and dirty energy sources.

4.2 Results

4.2.1 Carbon Taxes

We simulate the impact of a permanent and unexpected 50% value-added tax on dirty energy ($\tau_d = 0.50$). Casey et al. (2023) find that this is roughly the value of the best constant carbon tax in the GHKT special case with a climate externality calibrated to the social cost of carbon (SCC) calculations of Rennert et al. (2022a). We compare the predictions of our calibrated model to the GHKT special case ($\phi = 0$ and $\epsilon = 1$). Other than the differences in ϵ and ϕ, the two models are identical. For each model, we compare outcomes with the dirty energy tax to the laissez-faire equilibrium.

Figure 3 shows the results. Panel (a) shows dynamics of the energy expenditure share. As expected, they are qualitatively similar to those in Figure 2. In the period that policy is introduced, the energy expenditure share jumps almost one-for-one with the change in the tax-inclusive price of energy. In the GHKT special case, by contrast, the expenditure share is unchanged. Panel (b) shows the implications for the energy intensity of output, $s_{E,t}/p_{E,t}$, which is the inverse of economy-wide energy efficiency. The two models have identical long-run predictions, but different predictions for many decades after the introduction of the policy.

Next we turn to discussing the environmental implications of these results. In the period that policy is introduced, there is a 5 percent reduction in final energy use in our model (panel c). By contrast, energy use immediately drops by almost 28 percent in the GHKT special case. Over time, the two models converge to the lower GHKT level. Panel (d) translates these effects to dirty energy, rather than final use energy. The dynamics are similar, but muted because we assume the substitution between clean and dirty energy can happen instantaneously.

Panel (e) translates these effects to differences in cumulative dirty energy use, the variable most relevant for environmental outcomes. In the GHKT model, the tax reduces dirty energy use by roughly 35 percent, and this effect is constant over time. In our model, cumulative dirty energy use is only 19 percent below the laissez-fire level in 2030. This highlights a key implication of our findings. When examining the impact of climate-policy on medium-run outcomes, it is important to account for transition dynamics. Models that are only calibrated to long-run data will overstate the impact of policy on emissions. By 2100, our model predicts a 28 percent drop, which is more similar to the GHKT results. This similarity implies that the 80 year horizon is long enough for the medium-run dynamics to be mostly overwhelmed the long-run outcomes in determining cumulative emissions.

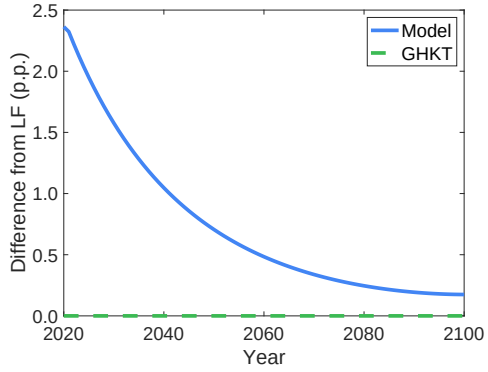

(a) Energy Expenditure Share

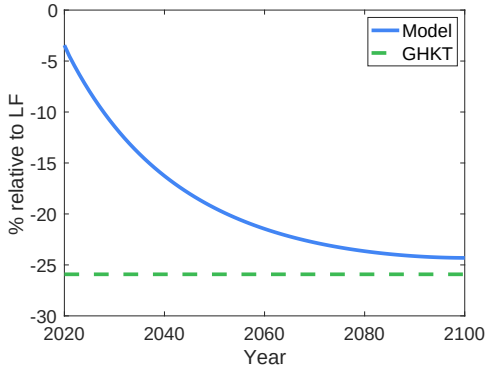

(b) Energy Intensity

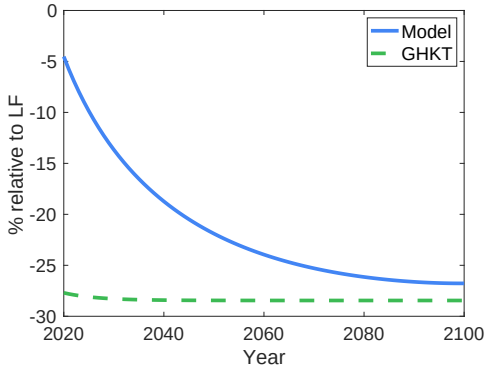

(c) Final Energy

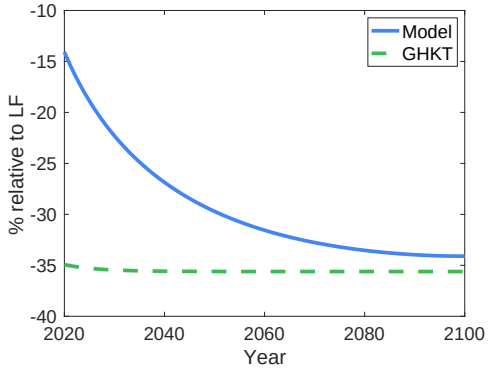

(d) Flow Dirty Energy

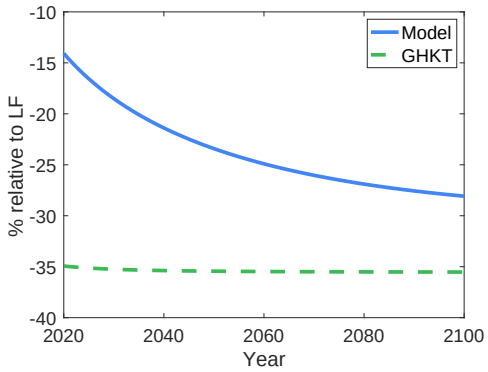

(e) Cumulative Dirty Energy

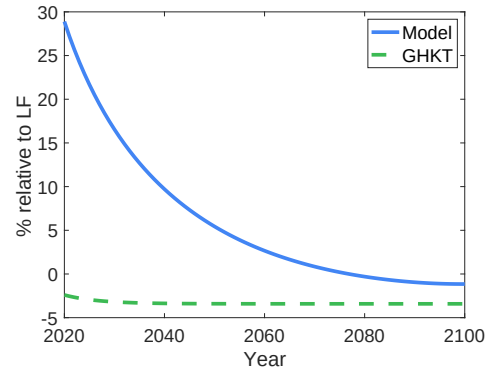

(f) Flow Clean Energy

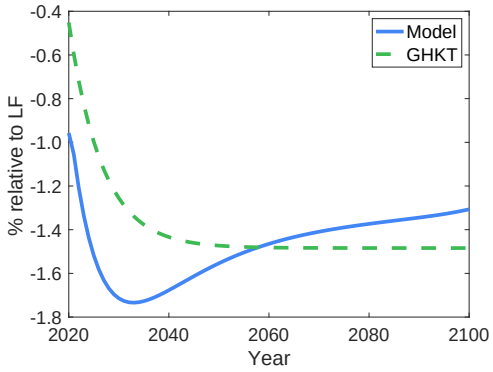

(g) GDP

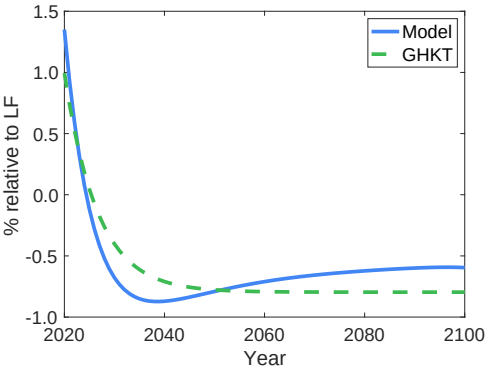

(h) Consumption

Figure 3: Impacts of a 50% Carbon Tax

For completeness, panel (f) presents the dynamics of clean energy use. Interestingly, the pattern of clean energy use is quite different in the two models. In our model, the demand for final energy is essentially unchanged in the period that policy is introduced, but the price of clean energy decreases relative to dirty energy. As a result, clean energy use spikes. In the GHKT model, by contrast, there is a significant reduction in the demand for energy use. Indeed, even though there is substitution away from dirty and towards clean, overall clean energy use decreases. Casey et al. (2023) provide a simple explanation for this result. They show that, in the GHKT framework, clean and dirty energy are gross complements. When a carbon tax decreases dirty energy use, it also decreases the return to extracting clean energy, leading to lower clean energy use. Our model shows that, while this may be true in the long run, the short- and medium-run dynamics are very different. We discuss the implications of this difference further when simulating the impacts of clean energy subsidies.

Finally, we turn to the macro aggregates. The two models yield similar predictions for the dynamics of output and consumption as shown in panel (h). The representative household responds by lowering the savings rate, leading to an initial spike in consumption and then a swift decline. While we have not conducted a welfare analysis, the results suggest that the welfare benefits of policy are smaller in our model. The paths of consumption are similar in the two models, but the environmental benefits are much lower when accounting for the slow energy efficiency dynamics. The long-run prediction for output are similar, as shown in panel (g), but the initial decline is much greater in our model. Our model captures the fact that the economy is less flexible in the short-run and firms cannot avoid paying high energy costs, which do not contribute to GDP.

4.2.2 Clean Energy Subsidies

In this section, we investigate the results of a clean energy subsidy, rather than a dirty energy tax. We focus on the case of a 20% subsidy ($\tau_c = 0.20$), which is roughly in line with the subsidies in the Inflation Reduction Act (Bistline et al., forthcoming). Unlike carbon taxes, clean energy subsidies decrease the price of energy and discourage energy efficiency (e.g., Newell et al., 2019). Thus, these policies are *more* effective when accounting for the slow dynamics of energy efficiency.

Figure 4 shows the results. As expected, panel (a) shows that subsidies cause the energy expenditure share to fall in the short run, because the elasticity of substitution is below one. As in the case of carbon taxes, the transition back to the original expenditure share happens very slowly. Panels (b) and (c) show the slow dynamics of energy intensity and final energy

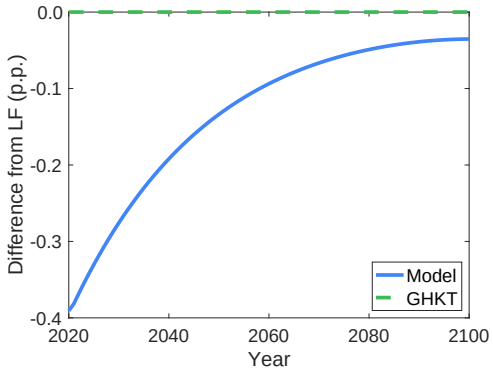

(a) Energy Expenditure Share

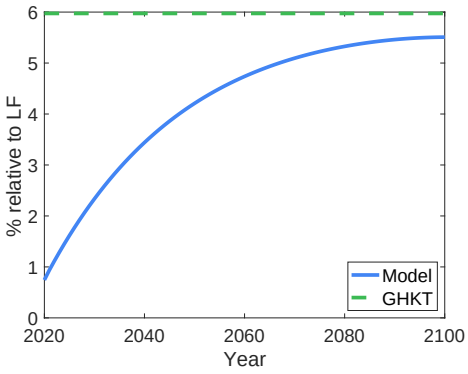

(b) Energy Intensity

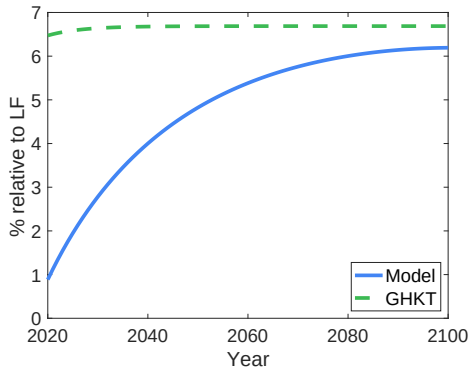

(c) Final Energy

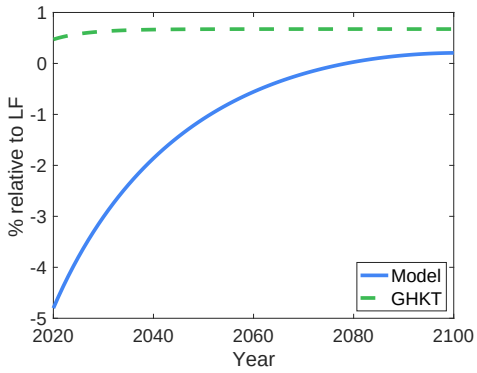

(d) Flow Dirty Energy

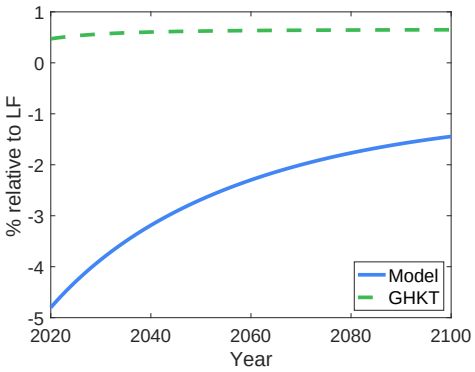

(e) Cumulative Dirty Energy

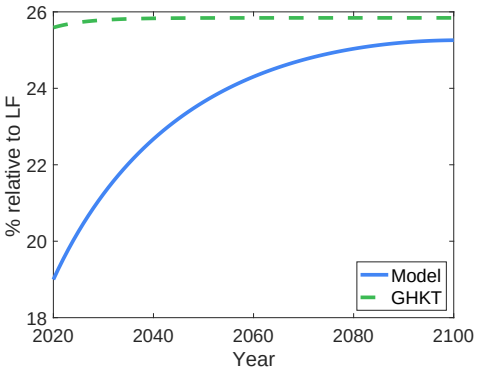

(f) Flow Clean Energy

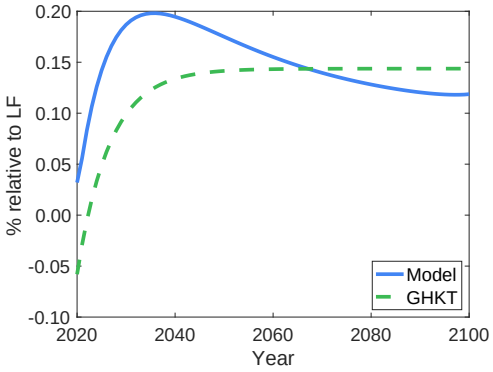

(g) GDP

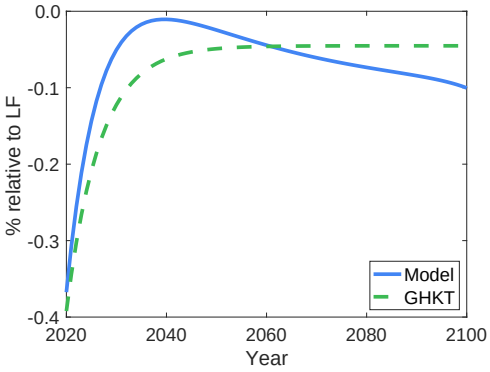

(h) Consumption

Figure 4: Impacts of a 20% Clean Energy Subsidy

use.

Panels (d) and (e) show the dynamics of flow and cumulative dirty energy use, respectively. Casey et al. (2023) show that clean energy subsidies actually *increase* emissions in the GHKT special case. While we find identical long-run results, our results suggest that clean energy subsidies are much more effective when taking into account the slow dynamics of energy use. The subsidies decrease flow dirty energy use by 5 percent in the short run and 1 percent in 2050. While the results still suggest limited effectiveness of these policies in reducing dirty energy use, the results also suggest that subsidies are unlikely to exacerbate environmental outcomes in the short run. More generally, the results again demonstrate the importance of accounting for slow energy transition dynamics when simulating the impacts of climate policy.

Panels (g) and (h) show the paths of GDP and consumption. The subsidy increases energy production, boosting GDP. But, it does so at the cost of decreasing consumption, at least partially offsetting the benefit of reduced emissions. This negative impact on consumption is expected, because laissez-faire equilibrium maximizes the utility from consumption.

5 Conclusion

Macro climate-economy models are powerful tools for studying climate policy. Indeed, Hassler et al. (2018) argue that macro climate-economy models are "the only game in town" (p. 391). Do current iterations of these models generate reasonable predictions that are useful inputs to policy decisions? Given the importance of these models, surprisingly little work has been done to compare their predictions to data.

In this paper, we compare the models to data with a focus on one important determinant of carbon emissions: economy-wide energy efficiency. To do so, we borrow an approach frequently used in the business cycle literature. We estimate impulse response functions in data and compare them to the model predictions. We then build a new model that nests the existing literature and can replicate these empirical observations.

We use the new model to study the impacts of climate policy. Our model suggests that the impact of a given carbon tax on cumulative carbon emissions will be smaller than commonly believed. Carbon taxes increase the price of energy and promote energy efficiency. The data and our model suggest that this process happens slowly over time, while older models assume that it happens instantaneously. We find the opposite results for clean energy subsidies. Since clean energy subsidies decrease energy prices, they are more effective when energy efficiency

dynamics are slow.

We have focused on a simple and transparent model to highlight our key findings regarding the dynamics of energy efficiency. We hope that our results will contribute to the broader research program of using macro climate-economy models to study climate change. Given the tractability of our model, future work can integrate our insights into full quantitative integrated assessment model (IAMs) that can be used to study optimal climate policy.

References

Adjemian, S., H. Bastani, M. Juillard et al. (2011): "Dynare: Reference Manual Version 4," Dynare Working Papers 1, CEPREMAP.

Airaudo, F. S., E. Pappa, and H. D. Seoane (2023): "The green metamorphosis of a small open economy."

André, F. J., and S. Smulders (2014): "Fueling growth when oil peaks: Directed technological change and the limits to efficiency," *European Economic Review*, 69, 18–39.

Annicchiarico, B., and F. Di Dio (2015): "Environmental policy and macroeconomic dynamics in a new Keynesian model," *Journal of Environmental Economics and Management*, 69, 1–21.

Atkeson, A., and P. J. Kehoe (1999): "Models of energy use: Putty-putty versus putty-clay," *American Economic Review*, 89, 1028–1043.

Auffhammer, M. (2018): "Quantifying economic damages from climate change," *Journal of Economic Perspectives*, 32, 33–52.

Barrage, L. (2020): "Optimal dynamic carbon taxes in a climate–economy model with distortionary fiscal policy," *Review of Economic Studies*, 87, 1–39.

Barrage, L., and W. D. Nordhaus (2023): "Policies, Projections, and the Social Cost of Carbon: Results from the DICE-2023 Model," *NBER Working Paper*.

Berndt, E. R., and D. O. Wood (1975): "Technology, prices, and the derived demand for energy," *Review of Economics and Statistics*, 259–268.

Bilal, A., and E. Rossi-Hansberg (2023): "Anticipating Climate Change Across the United States,"Technical report, National Bureau of Economic Research.

Bistline, J., N. Mehrotra, and C. Wolfram (forthcoming): "Economic Implications of the Climate Provisions of the Inflation Reduction Act," *Brookings Papers on Economic Activity*.

Blanchard, O. J., and D. Quah (1989): "The Dynamic Effects of Aggregate Demand and Supply Disturbances," *American Economic Review*, 655–673.

Campiglio, E., S. Dietz, and F. Venmans (2022): "Optimal climate policy as if the transition matters."

Casey, G. (2024): "Energy efficiency and directed technical change: implications for climate change mitigation," *Review of Economic Studies*, 91, 192–228.

Casey, G., and Y. Gao (2023): "Some Macroeconomic Evidence on Substitution between Clean and Dirty Energy," *Working Paper*.

Casey, G., W. Jeon, and C. Traeger (2023): "The Macroeconomics of Clean Energy Subsidies," *Working Paper*.

Cruz, J.-L., and E. Rossi-Hansberg (2024): "The economic geography of global warming," *Review of Economic Studies*, 91, 899–939.

Energy Information Administration (2023a): "Monthly Energy Review," https://www.eia.gov/totalenergy/data/monthly/ (accessed July 2023).

——— (2023b): "State Energy Data System," https://www.eia.gov/state/seds/seds-data-complete.php (accessed July 2023).

Feenstra, R. C., R. Inklaar, and M. P. Timmer (2015): "The Next Generation of the Penn World Table," *American Economic Review*, 105, 3150–3182.

Golosov, M., J. Hassler, P. Krusell, and A. Tsyvinski (2014): "Optimal taxes on fossil fuel in general equilibrium," *Econometrica*, 82, 41–88.

Griffin, J. M., and P. R. Gregory (1976): "An intercountry translog model of energy substitution responses," *American economic review*, 66, 845–857.

Hassler, J., and P. Krusell (2018): "Environmental macroeconomics: the case of climate change," in *Handbook of environmental economics* Volume 4: Elsevier, 333–394.

Hassler, J., P. Krusell, and C. Olovsson (2018): "The Consequences of Uncertainty: Climate Sensitivity and Economic Sensitivity to the Climate," *Annual Review of Economics*, 10, 189–205.

——— (2021a): "Directed technical change as a response to natural resource scarcity," *Journal of Political Economy*, 129, 3039–3072.

——— (2021b): "Suboptimal Climate Policy," *Journal of the European Economic Association*.

Hassler, J., P. Krusell, and A. A. Smith Jr (2016): "Environmental macroeconomics," in *Handbook of Macroeconomics* Volume 2: Elsevier, 1893–2008.

Heutel, G. (2012): "How should environmental policy respond to business cycles? Optimal policy under persistent productivity shocks," *Review of Economic Dynamics*, 15, 244–264.

Hinkelmann, S. (2023): "(Be-)Coming Clean: A model of the US Energy Transition," *Working Paper*.

——— (2024): "(Electrification of U.S. Aggregate Production: Evidence and Model," *Working Paper*.

Hinkelmann, S., and M. Farajpour (2021): "Climate Policies and Input Substitutability Over Time," *Working Paper*.

Holland, S. P., J. E. Hughes, and C. R. Knittel (2009): "Greenhouse gas reductions under low carbon fuel standards?" *American Economic Journal: Economic Policy*, 1, 106–46.

Jones, C. I. (2016): "The facts of economic growth," in *Handbook of Macroeconomics* Volume 2: Elsevier, 3–69.

Känzig, D. R. (2023): "The unequal economic consequences of carbon pricing," *Working Paper*.

Klenow, P., I. Nath, and V. Ramey (2023): "How much will global warming cool global growth," *NBER Working paper*.

Koetse, M. J., H. L. De Groot, and R. J. Florax (2008): "Capital-energy substitution and shifts in factor demand: A meta-analysis," *Energy Economics*, 30, 2236–2251.

Le Quéré, C., J. I. Korsbakken, C. Wilson et al. (2019): "Drivers of declining CO_2 emissions in 18 developed economies," *Nature Climate Change*, 9, 213–217.

Leon-Ledesma, M. A., and M. Satchi (2019): "Appropriate Technology and Balanced Growth," *Review of Economic Studies*, 86, 807–835.

Metcalf, G. E., and J. H. Stock (2023): "The macroeconomic impact of Europe's carbon taxes," *American Economic Journal: Macroeconomics*, 15, 265–286.

Newell, R. G., W. A. Pizer, and D. Raimi (2019): "US federal government subsidies for clean energy: Design choices and implications," *Energy Economics*, 80, 831–841.

Nordhaus, W. D. (1993): "Optimal greenhouse-gas reductions and tax policy in the DICE model," *American Economic Review*, 313–317.

Nordhaus, W. D., and J. Boyer (2000): *Warming the world: Economic models of global warming*: MIT press.

Peters, G. P., R. M. Andrew, J. G. Canadell, S. Fuss, R. B. Jackson, J. I. Korsbakken, C. Le Quéré, and N. Nakicenovic (2017): "Key indicators to track current progress and future ambition of the Paris Agreement," *Nature Climate Change*, 7, 118.

Pindyck, R. S. (1979): "Interfuel substitution and the industrial demand for energy: an international comparison," *Review of Economics and Statistics*, 169–179.

Pindyck, R. S., and J. J. Rotemberg (1983): "Dynamic factor demands and the effects of energy price shocks," *American Economic Review*, 73, 1066–1079.

Raupach, M. R., G. Marland, P. Ciais, C. Le Quéré, J. G. Canadell, G. Klepper, and C. B. Field (2007): "Global and regional drivers of accelerating CO_2 emissions," *Proceedings of the National Academy of Sciences*, 104, 10288–10293.

Rennert, K., F. Errickson, B. C. Prest et al. (2022a): "Comprehensive evidence implies a higher social cost of CO2," *Nature*, 610, 687–692.

Rennert, K., B. C. Prest, W. A. Pizer et al. (2022b): "The social cost of carbon: advances in long-term probabilistic projections of population, GDP, emissions, and discount rates," *Brookings Papers on Economic Activity*, 2021, 223–305.

Smith, A. (2008): "Indirect inference," *The New Palgrave Dictionary of Economics, 2nd Edition (forthcoming)*.

University of Groningen and University of California, Davis (2024): "Total Factor Productivity at Constant National Prices for United States [RTFPNAUSA632NRUG]," https://fred.stlouisfed.org/series/RTFPNAUSA632NRUG (retrieved from FRED, Federal Reserve Bank of St. Louis; accessed 8/13/24).

Van der Werf, E. (2008): "Production functions for climate policy modeling: An empirical analysis," *Energy Economics*, 30, 2964–2979.

Online Appendix

Energy Efficiency Dynamics and Climate Policy

By: Gregory Casey and Yang Gao

A Model Analysis

A.1 Characterization of Competitive Equilibrium

A.1.1 Final Good Producer Problem

The firm's problem is

$$\max_{\{N_t,E_t,\theta_{t+1}\}_{t=0}^{\infty}} \mathbb{E}_0 \sum_{t=0}^{\infty} \left[\prod_{\tilde{t}=0}^{t} \Lambda_{\tilde{t}}\right] \times \left[\left(1-\frac{\phi}{2}\left(\frac{\theta_t}{\theta_{t-1}}-1\right)^2\right) \underbrace{X_t\left(\left(\theta_t^{-\eta}N_t\right)^{\frac{\epsilon-1}{\epsilon}}+\left(\theta_t^{1-\eta}E_t\right)^{\frac{\epsilon-1}{\epsilon}}\right)^{\frac{\epsilon}{\epsilon-1}}}_{\tilde{Y}_t} - p_{N,t}N_t - p_{E,t}E_t\right], \tag{A.1}$$

where θ_0 and θ_{-1} are given and it discounts future profits using household's stochastic discount factor, $\Lambda_{t+1} \equiv \beta\frac{u'(C_{t+1})}{u'(C_t)} = \beta\frac{C_t}{C_{t+1}}$. The first order conditions are

$$N_t: \quad \frac{p_{N,t}N_t}{\tilde{Y}_t} = \left(1-\frac{\phi}{2}\left(\frac{\theta_t}{\theta_{t-1}}-1\right)^2\right)\left(\frac{\tilde{Y}_t}{N_t}\right)^{\frac{1-\epsilon}{\epsilon}}\left(X_t\theta_t^{-\eta}\right)^{\frac{\epsilon-1}{\epsilon}} \tag{A.2}$$

$$E_t: \quad \frac{p_{E,t}E_t}{\tilde{Y}_t} = \left(1-\frac{\phi}{2}\left(\frac{\theta_t}{\theta_{t-1}}-1\right)^2\right)\left(\frac{\tilde{Y}_t}{E_t}\right)^{\frac{1-\epsilon}{\epsilon}}\left(X_t\theta_t^{1-\eta}\right)^{\frac{\epsilon-1}{\epsilon}} \tag{A.3}$$

$$\begin{aligned}\theta_{t+1}: \quad 0 =& \mathbb{E}_t\Bigg\{-\phi\left(\frac{\theta_{t+1}}{\theta_t}-1\right)\frac{\theta_{t+1}}{\theta_t} \\ &+\Lambda_{t+2}\phi\left(\frac{\theta_{t+2}}{\theta_{t+1}}-1\right)\frac{\theta_{t+2}}{\theta_{t+1}}\frac{\tilde{Y}_{t+2}}{\tilde{Y}_{t+1}} \\ &+\left(1-\frac{\phi}{2}\left(\frac{\theta_{t+1}}{\theta_t}-1\right)^2\right)\left(\frac{\tilde{Y}_{t+1}}{X_{t+1}}\right)^{\frac{1-\epsilon}{\epsilon}} \\ &\times\left[-\eta\left(\theta_{t+1}^{-\eta}N_{t+1}\right)^{\frac{\epsilon-1}{\epsilon}}+(1-\eta)\left(\theta_{t+1}^{1-\eta}E_{t+1}\right)^{\frac{\epsilon-1}{\epsilon}}\right]\Bigg\}.\end{aligned} \tag{A.4}$$

Combining all of the first-order conditions, we can re-write the last (A.4) as

$$\begin{aligned}\theta_{t+1}: \quad 0 =& \mathbb{E}_t\Bigg\{-\phi\left(\frac{\theta_{t+1}}{\theta_t}-1\right)\frac{\theta_{t+1}}{\theta_t} \\ &+\Lambda_{t+2}\phi\left(\frac{\theta_{t+2}}{\theta_{t+1}}-1\right)\frac{\theta_{t+2}}{\theta_{t+1}}\frac{\tilde{Y}_{t+2}}{\tilde{Y}_{t+1}} \\ &+\left(1-\frac{\phi}{2}\left(\frac{\theta_{t+1}}{\theta_t}-1\right)^2\right)\left[-\eta s_{N,t+1}+(1-\eta)s_{E,t+1})\right]\Bigg\},\end{aligned} \tag{A.5}$$

where $s_{J,t}=\frac{p_{J,t}J_t}{\left(1-\Phi\left(\frac{\theta_t}{\theta_{t-1}}\right)\right)\tilde{Y}_t}$ is share of output paid to factor $J=N,E$ and $s_{N,t}+s_{E,t}=1$. Plugging this identity into the previous equation and rearranging yields

$$\begin{aligned}\theta_{t+1}: \quad 0 =& \mathbb{E}_t\Bigg\{-\phi\left(\frac{\theta_{t+1}}{\theta_t}-1\right)\frac{\theta_{t+1}}{\theta_t} \\ &+\Lambda_{t+2}\phi\left(\frac{\theta_{t+2}}{\theta_{t+1}}-1\right)\frac{\theta_{t+2}}{\theta_{t+1}}\frac{\tilde{Y}_{t+2}}{\tilde{Y}_{t+1}} \\ &-\frac{p_{N,t+1}N_{t+1}}{\tilde{Y}_{t+1}}+(1-\eta)\left(1-\frac{\phi}{2}\left(\frac{\theta_{t+1}}{\theta_t}-1\right)^2\right)\Bigg\}.\end{aligned} \tag{A.6}$$

A.1.2 Intermediate Producer Problem

The intermediate producer solves

$$\max_{K_t,L} \quad p_{N,t}K_t^{\alpha}L^{1-\alpha}-\rho_t K_t - w_t L, \tag{A.7}$$

which gives

$$\rho_t = \alpha p_{N,t}K_t^{\alpha-1}L^{1-\alpha} \tag{A.8}$$

$$w_t = (1-\alpha)p_{N,t}K_t^{\alpha}L^{-\alpha}. \tag{A.9}$$

Combining these results gives the usual price index:

$$p_{N,t} = \alpha^{-\alpha}(1-\alpha)^{\alpha-1}w_t^{1-\alpha}\rho_t^{\alpha}. \tag{A.10}$$

A.1.3 Household Problem

The household maximizes (9) subject to the budget constraint given by (10) and (11), which yields the Euler equation,

$$1 = \mathbb{E}_t \left(\beta \frac{C_t}{C_{t+1}} (1 + \rho_{t+1} - \delta) \right), \tag{A.11}$$

and the transversality condition,

$$\lim_{T \to \infty} \mathbb{E}_T \left(\beta^T C_T^{-1} K_{T+1} \right) = 0. \tag{A.12}$$

A.2 Proof of Proposition 1

To derive the results, we consider the first order conditions from our fully-specified model, but consider the case where there are no adjustment costs ($\phi = 0$), which implies that firms maximize single-period profits.

To find the σ_{SR}, we combine (A.2) and (A.3) to get

$$E_t / N_t = (p_{E,t} / p_{N,t})^{-\epsilon} \theta_t^{\epsilon - 1} \tag{A.13}$$

and then compute

$$\sigma_{SR} := - \frac{d \ln(\frac{E_t}{N_t})}{d \ln(\frac{p_{E,t}}{p_{N,t}})} \bigg|_{\theta_t \text{ fixed}} = \epsilon. \tag{A.14}$$

To find σ_{LR}, we evaluate the combined first-order condition (A.5) with $\phi = 0$:

$$E_t / N_t = \frac{\eta}{1 - \eta} \left(\frac{p_{E,t}}{p_{N,t}} \right)^{-1}. \tag{A.15}$$

and compute

$$\sigma_{LR} := - \frac{d \ln(\frac{E_t}{N_t})}{d \ln(\frac{p_{E,t}}{p_{N,t}})} = 1. \tag{A.16}$$

A.3 Intensive Form

In this section, we present the intensive form of the model. We use $\widehat{Z}_t \equiv Z_t / \overline{Z_t}$ to denote the de-trended value for any variables Z_t and $\kappa_{Z,t} \equiv Z_t / Z_{t-1}$ to denote the ratio of current

to last period level of any variable Z_t.

The trend for $C_t, I_t, \tilde{Y}_t, w_t$ is defined by $\overline{\tilde{Y}_t} = X_t^{\frac{1}{(1-\alpha)(1-\eta)}} p_{E,t}^{\frac{-\eta}{(1-\alpha)(1-\eta)}}$. The trends for E_t and N_t are defined by $\overline{E_t} = X_t^{\frac{1}{(1-\alpha)(1-\eta)}} p_{E,t}^{\frac{\alpha(1-\eta)-1}{(1-\alpha)(1-\eta)}}$ and $\overline{N_t} = X_t^{\frac{\alpha}{(1-\alpha)(1-\eta)}} p_{E,t}^{\frac{-\alpha\eta}{(1-\alpha)(1-\eta)}}$ respectively. The trends for K_t and θ_t are defined by $\overline{K_t} = X_{t-1}^{\frac{1}{(1-\alpha)(1-\eta)}} p_{E,t-1}^{\frac{-\eta}{(1-\alpha)(1-\eta)}}$ and $\overline{\theta_t} = X_{t-1}^{\frac{-1}{1-\eta}} p_{E,t-1}^{\frac{1}{1-\eta}}$ respectively. Lastly, the trend for $p_{N,t}$ is defined by $\overline{p_{N,t}} = X_t^{\frac{1}{1-\eta}} p_{E,t}^{\frac{-\eta}{1-\eta}}$. Equations (A.17) to (A.30) describe the full competitive equilibrium in intensive form:

$$exp\left(g_{X,t}\frac{1}{(1-\alpha)(1-\eta)}\right) exp\left(g_{p_{E,t}}\frac{-\eta}{(1-\alpha)(1-\eta)}\right) = \kappa_{\tilde{Y},t} \tag{A.17}$$

$$exp\left(g_{X,t-1}\frac{-1}{1-\eta}\right) exp\left(g_{p_{E,t-1}}\frac{1}{1-\eta}\right) = \kappa_{\theta,t} \tag{A.18}$$

$$\Lambda_{t+1} \equiv \beta \frac{\widehat{C}_t}{\widehat{C}_{t+1}\kappa_{\tilde{Y},t+1}} \tag{A.19}$$

$$\mathbb{E}_t\left[\Lambda_{t+1}(1+\rho_{t+1}-\delta)\right] = 1 \tag{A.20}$$

$$\left(\left(\widehat{\theta}_t^{-\eta}\widehat{N}_t\kappa_{\theta,t+1}^{\eta}\right)^{\frac{\epsilon-1}{\epsilon}} + \left(\widehat{\theta}_t^{1-\eta}\widehat{E}_t\kappa_{\theta,t+1}^{\eta-1}\right)^{\frac{\epsilon-1}{\epsilon}}\right)^{\frac{\epsilon}{\epsilon-1}} = \widehat{\tilde{Y}}_t \tag{A.21}$$

$$\begin{aligned}\mathbb{E}_t\Bigg\{(1-\eta)\left[1-\Phi\left(\frac{\widehat{\theta}_{t+1}}{\widehat{\theta}_t}\kappa_{\theta,t+1}\right)\right] - \frac{\widehat{p}_{N,t+1}\widehat{N}_{t+1}}{\widehat{\tilde{Y}}_{t+1}} \\ -\Phi'\left(\frac{\widehat{\theta}_{t+1}}{\widehat{\theta}_t}\kappa_{\theta,t+1}\right)\left(\frac{\widehat{\theta}_{t+1}}{\widehat{\theta}_t}\kappa_{\theta,t+1}\right) \\ +\Lambda_{t+2}\Phi'\left(\frac{\widehat{\theta}_{t+2}}{\widehat{\theta}_{t+1}}\kappa_{\theta,t+2}\right)\left(\frac{\widehat{\theta}_{t+2}}{\widehat{\theta}_{t+1}}\kappa_{\theta,t+2}\right)\frac{\widehat{\tilde{Y}}_{t+2}}{\widehat{\tilde{Y}}_{t+1}}\kappa_{\tilde{Y},t+2}\Bigg\} = 0\end{aligned} \tag{A.22}$$

$$\left[1-\Phi\left(\frac{\widehat{\theta}_t}{\widehat{\theta}_{t-1}}\kappa_{\theta,t}\right)\right]\left(\left(\frac{\widehat{\theta}_t}{\kappa_{\theta,t+1}}\right)^{1-\eta}\right)^{\frac{\epsilon-1}{\epsilon}}\left(\frac{\widehat{\tilde{Y}}_t}{\widehat{E}_t}\right)^{\frac{1}{\epsilon}}=1 \tag{A.23}$$

$$\left[1-\Phi\left(\frac{\widehat{\theta}_t}{\widehat{\theta}_{t-1}}\kappa_{\theta,t}\right)\right]\left(\left(\frac{\widehat{\theta}_t}{\kappa_{\theta,t+1}}\right)^{-\eta}\right)^{\frac{\epsilon-1}{\epsilon}}\left(\frac{\widehat{\tilde{Y}}_t}{\widehat{N}_t}\right)^{\frac{1}{\epsilon}}=\widehat{p}_{N,t} \tag{A.24}$$

$$\widehat{N}_t\kappa_{\tilde{Y},t}^{\alpha}=\widehat{K}_t^{\alpha} \tag{A.25}$$

$$\alpha\frac{\widehat{N}_t}{\widehat{K}_t}\kappa_{\tilde{Y},t}=\frac{\rho_t}{\widehat{p}_{N,t}} \tag{A.26}$$

$$(1-\alpha)\widehat{N}_t=\frac{\widehat{w}_t}{\widehat{p}_{N,t}} \tag{A.27}$$

$$\widehat{C}_t+\widehat{K}_{t+1}+\widehat{E}_t=\left[1-\Phi\left(\frac{\widehat{\theta}_t}{\widehat{\theta}_{t-1}}\kappa_{\theta,t}\right)\right]\widehat{\tilde{Y}}_t+(1-\delta)\widehat{K}_t\frac{1}{\kappa_{\tilde{Y},t}}. \tag{A.28}$$

$$(1-\rho_X)\mu_X+\rho_X g_{X,t-1}+\omega_{X,t}=g_{X,t}, \tag{A.29}$$

$$(1-\rho_{p_E})\mu_{p_E}+\rho_{p_E}g_{p_E,t-1}+\omega_{p_E,t}=g_{p_E,t} \tag{A.30}$$

A.4 Balanced Growth Path

We use Z_{ss} to denote the steady state value of any variable Z, which is frequently a detrended variable. The steady state of the full model is as follows:

$$\kappa_{\tilde{Y},ss}=exp\left(\mu_X\frac{1}{(1-\alpha)(1-\eta)}\right)exp\left(\mu_{p_E}\frac{-\eta}{(1-\alpha)(1-\eta)}\right) \tag{A.31}$$

$$\kappa_{\theta,ss}=exp\left(\mu_X\frac{-1}{1-\eta}\right)exp\left(\mu_{p_E}\frac{1}{1-\eta}\right) \tag{A.32}$$

$$\Phi_{ss}(\kappa_{\theta,ss})=\frac{\phi}{2}(\kappa_{\theta,ss}-1)^2 \tag{A.33}$$

$$\Phi'_{ss}(\kappa_{\theta,ss})=\phi(\kappa_{\theta,ss}-1) \tag{A.34}$$

$$\Lambda_{ss}=\beta/\kappa_{\tilde{Y},ss} \tag{A.35}$$

$$\rho_{ss}=\frac{1}{\Lambda_{ss}}-1+\delta \tag{A.36}$$

$$s_{N,ss}=1-\eta-\frac{\Phi'_{ss}(\kappa_{\theta,ss})\kappa_{\theta,ss}(1-\Lambda_{ss}\kappa_{\tilde{Y},ss})}{1-\Phi_{ss}(\kappa_{\theta,ss})} \tag{A.37}$$

$$s_{E,ss}=1-s_{N,ss} \tag{A.38}$$

$$\widehat{\theta}_{ss}=\kappa_{\theta,ss}\left((1-\Phi_{ss}(\kappa_{\theta,ss}))^{\frac{\epsilon-1}{\epsilon}}s_{E,ss}^{\frac{-1}{\epsilon}}\right)^{\frac{-\epsilon}{(\epsilon-1)(1-\eta)}} \tag{A.39}$$

$$\widehat{p}_{N,ss} = (1 - \Phi_{ss}(\kappa_{\theta,ss}))s_{N,ss}^{\frac{-1}{\epsilon-1}} \left(\frac{\widehat{\theta}_{ss}}{\kappa_{\theta,ss}} \right)^{-\eta} \tag{A.40}$$

$$\widehat{K}_{ss} = \left(\frac{\alpha \widehat{p}_{N,ss}}{\rho_{ss}} \right)^{\frac{1}{1-\alpha}} \kappa_{\tilde{Y},ss} \tag{A.41}$$

$$\widehat{I}_{ss} = \left(1 - \frac{1-\delta}{\kappa_{\tilde{Y},ss}} \right) \widehat{K}_{ss} \tag{A.42}$$

$$\widehat{N}_{ss} = \left(\frac{\widehat{K}_{ss}}{\kappa_{\tilde{Y},ss}} \right)^{\alpha} \tag{A.43}$$

$$\widehat{w}_{ss} = (1-\alpha)\widehat{N}_{ss}\widehat{p}_{N,ss} \tag{A.44}$$

$$\widehat{\tilde{Y}}_{ss} = \frac{\widehat{p}_{N,ss}\widehat{N}_{ss}}{(1 - \Phi_{ss}(\kappa_{\theta,ss}))s_{N,ss}} \tag{A.45}$$

$$\widehat{E}_{ss} = \widehat{\tilde{Y}}_{ss} s_{E,ss}(1 - \Phi_{ss}(\kappa_{\theta,ss})) \tag{A.46}$$

$$\widehat{C}_{ss} = (1 - \Phi_{ss}(\kappa_{\theta,ss}))\widehat{\tilde{Y}}_{ss} - \widehat{I}_{ss} - \widehat{E}_{ss}. \tag{A.47}$$

A.5 Clean and Dirty Energy in Model with Deterministic Growth

To induce stationarity in the extended deterministic model with clean and dirty energy, the trends for the price of final energy as well as clean and dirty energy use are defined by $\overline{p_{E,t}} = p_{c,t}^{1-\gamma} p_{d,t}^{\gamma}$, $\overline{E_{c,t}} = X_t^{\frac{1}{(1-\alpha)(1-\eta)}} p_{c,t}^{\frac{-\eta(1-\gamma)-(1-\alpha)(1-\eta)}{(1-\alpha)(1-\eta)}} p_{d,t}^{\frac{-\eta\gamma}{(1-\alpha)(1-\eta)}}$ and $\overline{E_{d,t}} = X_t^{\frac{1}{(1-\alpha)(1-\eta)}} p_{c,t}^{\frac{-\eta(1-\gamma)}{(1-\alpha)(1-\eta)}} p_{d,t}^{\frac{-\eta\gamma-(1-\alpha)(1-\eta)}{(1-\alpha)(1-\eta)}}$, respectively. Then the intensive form of both equation (21) and the first-order conditions associated with the final energy production (20) can be written as:

$$\widehat{p}_{E,t} = \tilde{\gamma}(1 - \tau_{c,t})^{1-\gamma}(1 + \tau_{d,t})^{\gamma} \tag{A.48}$$

$$(1 - \tau_{c,t})\widehat{E}_{c,t} = (1-\gamma)\widehat{p}_{E,t}\widehat{E}_t \tag{A.49}$$

$$(1 + \tau_{d,t})\widehat{E}_{d,t} = \gamma \widehat{p}_{E,t}\widehat{E}_t. \tag{A.50}$$

The steady state value of the related variables are:

$$\widehat{p}_{E,ss} = \tilde{\gamma}(1 - \tau_{c,ss})^{1-\gamma}(1 + \tau_{d,ss})^{\gamma} \tag{A.51}$$

$$\widehat{E}_{c,ss} = \frac{(1-\gamma)\widehat{p}_{E,ss}\widehat{E}_{ss}}{1 - \tau_{c,ss}} \tag{A.52}$$

$$\widehat{E}_{d,ss} = \frac{\gamma \widehat{p}_{E,ss}\widehat{E}_{ss}}{1 + \tau_{d,ss}}. \tag{A.53}$$

In addition, when moving to a deterministic model with multiple types of energy, all growth terms ($\kappa_{Z,t}$) remain unchanged over time and the following dynamic equations need to be updated relative to their stochastic versions in Appendix Section A.3:

$$\left[1-\Phi\left(\frac{\widehat{\theta}_t}{\widehat{\theta}_{t-1}}\kappa_{\theta,t}\right)\right]\left(\left(\frac{\widehat{\theta}_t}{\kappa_{\theta,t+1}}\right)^{1-\eta}\right)^{\frac{\epsilon-1}{\epsilon}}\left(\frac{\widehat{\tilde{Y}}_t}{\widehat{E}_t}\right)^{\frac{1}{\epsilon}}=\widehat{p}_{E,t} \tag{A.54}$$

$$\widehat{C}_t+\widehat{K}_{t+1}+\widehat{E}_{c,t}+\widehat{E}_{d,t}=\left[1-\Phi\left(\frac{\widehat{\theta}_t}{\widehat{\theta}_{t-1}}\kappa_{\theta,t}\right)\right]\widehat{\tilde{Y}}_t+(1-\delta)\widehat{K}_t\frac{1}{\kappa_{\tilde{Y},t}}. \tag{A.55}$$

and the following steady state equations need to be updated relative to their values from Appendix Section A.4:

$$\widehat{\theta}_{ss}=\widehat{p}_{E,ss}^{\frac{1}{1-\eta}}\kappa_{\theta,ss}\left((1-\Phi_{ss}(\kappa_{\theta,ss}))^{\frac{\epsilon-1}{\epsilon}}s_{E,ss}^{\frac{-1}{\epsilon}}\right)^{\frac{-\epsilon}{(\epsilon-1)(1-\eta)}} \tag{A.56}$$

$$\widehat{E}_{ss}=\frac{\widehat{\tilde{Y}}_{ss}s_{E,ss}(1-\Phi_{ss}(\kappa_{\theta,ss}))}{\widehat{p}_{E,ss}} \tag{A.57}$$

$$\widehat{C}_{ss}=(1-\Phi_{ss}(\kappa_{\theta,ss}))\widehat{\tilde{Y}}_{ss}-\widehat{I}_{ss}-\widehat{E}_{c,ss}-\widehat{E}_{d,ss}. \tag{A.58}$$

A.6 Numerical Solution Method

We implement the model solution in *Dynare* (Adjemian et al., 2011). The stochastic model is solved with a first-order approximation of the model around its steady state. The deterministic model is solved with a perfect foresight solver given an initial and a terminal steady state.

B Data Sources

Unless otherwise noted, all of our data come from the State Energy Data System (SEDS) produced by the EIA (https://www.eia.gov/state/seds/seds-data-complete.php?sid=US). The data cover the period 1970-2021. All variable codes refer to these data. The codebook is available at https://www.eia.gov/state/seds/seds-technical-notes-complete.php?sid=US (see 'Codes and descriptions').

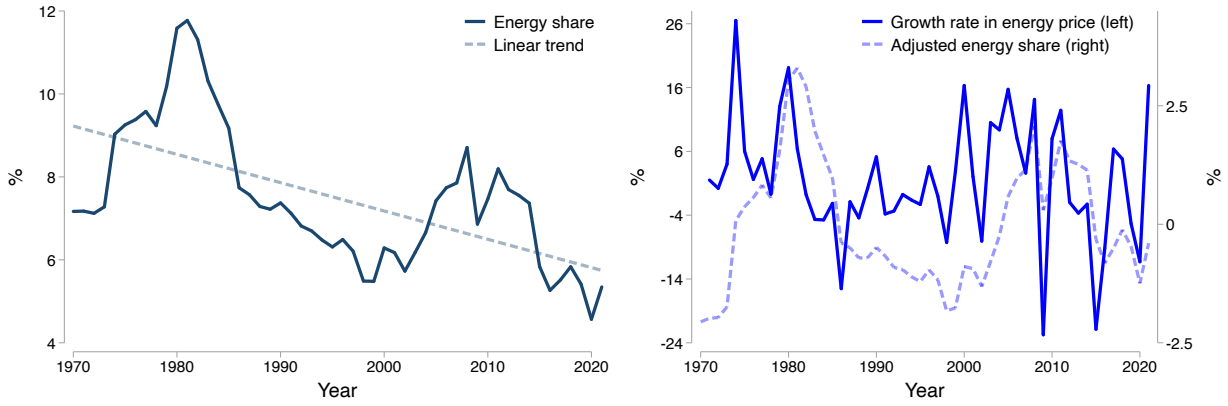

(a) Energy Share and Time Trend (b) Adjusted Share and Energy Price Growth

Figure B.1: Data Inputs into VAR

B.1 Data for Estimating IRFs

The SEDS data directly report total expenditure on final energy ('total end-use energy expenditures', TETXV) and the BTU-weighted nominal price of final energy ('total end-use energy average price', TETXD). Both are nominal values. The EIA also reports nominal GDP, real GDP, and the GDP deflator in its Monthly Economic Review (MER) data series (see Table C1 at https://www.eia.gov/totalenergy/data/monthly/). These data originally come from the Bureau of Economic Analysis (BEA). The energy expenditure share is total expenditure on final energy divided by the sum of nominal GDP and energy expenditure, and the real price of final energy is the nominal price divided by the GDP deflator. Real values are measured in 2012 dollars.

Prior to estimating the IRFs in the model, we separately estimate the dynamics of TFP. To do so, we use data on total factor productivity at constant national prices for United States from Federal Reserve Bank of St. Louis (https://fred.stlouisfed.org/series/RTFPNAUSA632NRUG). The TFP data series covers the period 1970-2019.

B.2 Transformed Data Used in VARs

Panel (a) of Figure B.1 shows the raw time series of energy expenditure share as well as a fitted linear time trend. Panel (b) shows the two data series used in our baseline analysis: the growth rate of energy prices and the de-trended energy expenditure share.

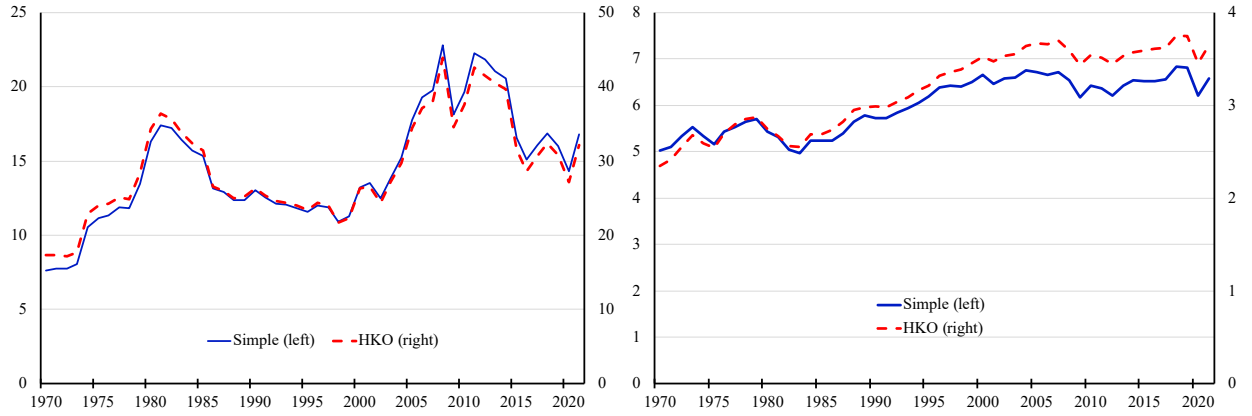

(a) Prices (b) Quantities

Figure B.2: Comparison to Hassler et al. (2021a) Measurement

Note: Panel (a) shows the average real price of final energy from the SEDS data ($2012/million BTUs) and the average real price of final energy using the HKO methodology ($2012/million BTUs of electricity). Panel (b) shows quantity of final energy from the SEDS data (billion BTUs) and using the HKO methodology (billion BTUs of electricity).

B.3 Comparison to Hassler et al. (2021a)

Hassler et al. (2021a) suggest an alternate method of estimating aggregate energy prices that weights different types of energy by their average price. They apply their method to fossil fuel primary energy. We recalculate our measure of the average real price of final energy and show that it is very similar to the series we use in our empirical analysis.

To do so, we consider final energy from four sources: electricity, coal, natural gas, and petroleum products. Coal and natural gas are considered final energy when they are not used to produce electricity (e.g., when they are used in industrial production or for residential heating). This analysis excludes final energy from biomass, because price data is unavailable. SEDS reports the nominal price of each energy type when it is used as a source of final energy (ESTXD, CLTXD, NGTXD, and PATXD). As above, we convert these to real values using the GDP deflator. On average, coal is 11% as expensive as electricity per BTU, while natural gas is 25% as expensive and petroleum products are 51% as expensive. The Hassler et al. (2021a) method assumes that these relative prices reflect differences in the relative efficiency of different energy sources. Then, we can calculate the total quantity of energy measured in BTUs of electricity as

$$E^{\text{HKO}} = E_e + 0.11E_c + 0.25E_g + 0.51E_p, \tag{B.1}$$

where E_e is BTUs of electricity used as a final energy source (ESTXB in the SEDS data), E_c is BTUs of coal (CLTXB), E_g is BTUs of natural gas (NGTXB), and E_p is BTUs of petroleum products (PATXB).

Note that the calculation of total expenditure on final energy is not affected by how we weight energy sources. The weighted-average real price of final energy can then be calculated as E^{HKO} divided by real expenditure on final energy:

$$p_E^{\text{HKO}} = \frac{p_E E}{E^{\text{HKO}}}, \tag{B.2}$$

where $p_E E$ is real energy expenditure. Panel (a) of B.2 plots the price series used in our analysis and the HKO version. While they have different units (BTUs versus BTUs of electricity), they move together very closely, indicating that our results are not driven by our method of calculating the average real price of final energy. For completeness, panel (b) plots total BTUs of final energy against E^{HKO} and shows that they also follow a similar path.

B.4 Additional Data for Policy Analyses

To conduct the policy analyses, we add substitution between clean and dirty sources of energy to the model. Calibrating the new parameters requires additional data on primary energy use and expenditure. To calculate total expenditure on fossil fuels, we sum total expenditure on coal (CLTCV), natural gas (NGTCV), and petroleum products (PATCV). Note that this includes coal and and natural gas used as final energy. When coal and natural gas are not altered prior to their use in production, they are both primary and final energy. We divide total expenditure on fossil fuels by total expenditure on final energy to estimate γ. Casey and Gao (2023) provide a more detailed analysis of substitution between clean and dirty sources of energy.

To measure the total quantity of dirty use, we add total consumption of coal (CLTCB), natural gas (NGTCB), and petroleum products (PATCB). As in our main calculation for final energy, we measure quantities in BTUs for all energy sources. To measure the average price of dirty energy, we divide expenditure on fossil fuels by total usage. We convert nominal prices to real prices using the GDP deflator. To measure the total quantity of clean energy, we take the total quantity of renewable energy directly from the data (RETCB).

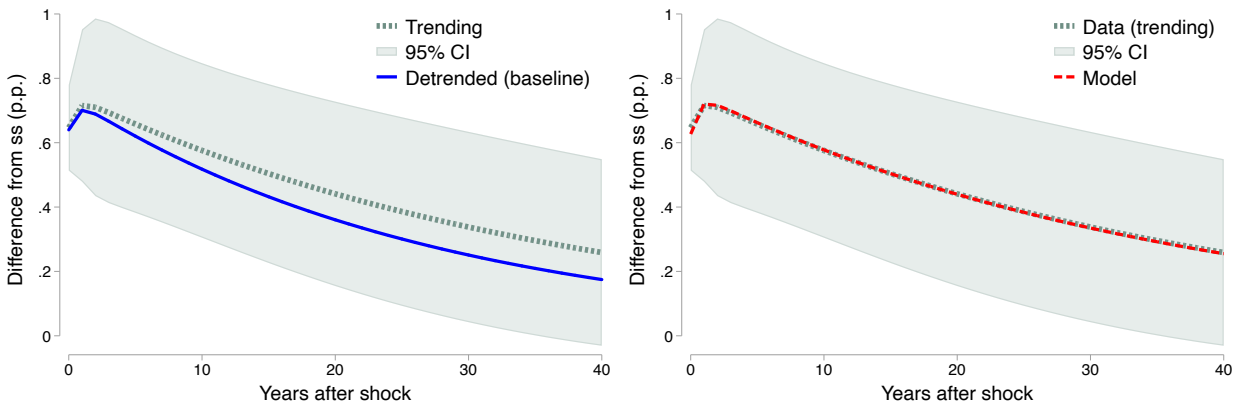

(a) Empirical IRFs (b) IRF Matching

Figure C.3: Results with Trending Data

C Robustness

C.1 Results without De-trending $s_{E,t}$

Our baseline results use the de-trended energy expenditure share. Our results are quantitatively and qualitatively similar when using the trending data. Panel (a) of Figure C.3 shows the empirical IRFs when using the trending data. Panel (b) of Figure C.3 plots the results of IRF matching using the trending data, which yields an $\epsilon = 0.17$ and $\phi = 54$ in the model (compared to $\epsilon = 0.14$ and $\phi = 32$ in the baseline specification). To recreate the slower transition dynamics, the model requires a higher ϕ to match the IRFs. To summarize, our decision to de-trend the energy expenditure share in the baseline results is conservative and has little effect on the results.

C.2 Empirical IRFs with Alternative Lag Order Selection

Table C.1 summarizes the results of lag order selection criteria for our SVAR specification. We show results varying the lag length for equation (19) while imposing that energy prices follow an exogenous AR(1) process. A lower FPE, AIC, BIC or HQIC value indicates a better fit. All statistics are consistent with an optimal lag order of 1. We obtain similar results when letting the lag length vary in both VAR equations.

Figure C.4 shows the IRFs with lag order of 3 and 5 in equation (19), while assuming energy prices follow an exogenous AR(1) process. The energy share response in both specifications is similar to our baseline results, indicating that our baseline results are robust.

Table C.1: Lag Order Selection Statistics

lag	FPE	AIC	BIC	HQIC
1	**2.40e-08***	**-11.83***	**-11.60***	**-11.74***
2	2.49e-08	-11.71	-11.33	-11.57
3	2.77e-08	-11.52	-10.97	-11.31
4	2.55e-08	-11.51	-10.81	-11.25
5	2.84e-08	-11.31	-10.44	-10.99

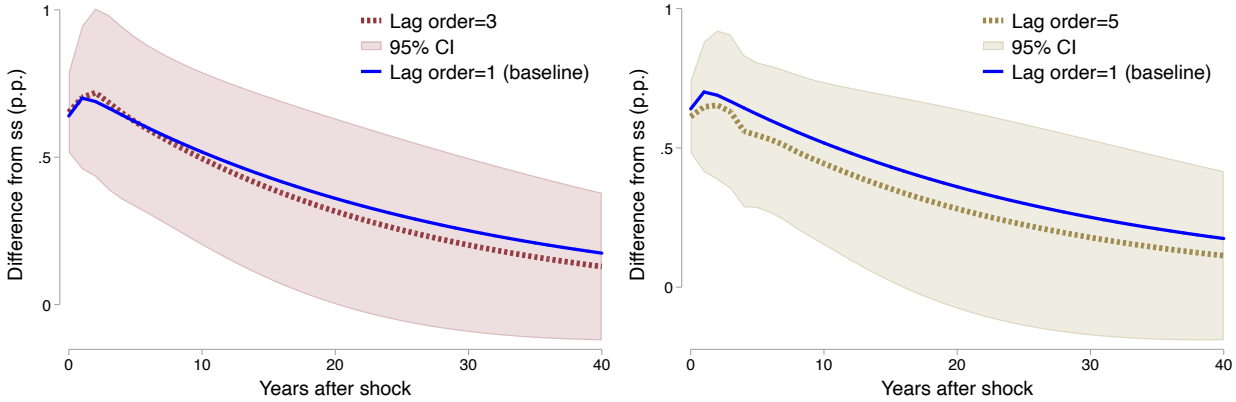

(a) Energy Share: Lag Order = 3

(b) Energy Share: Lag Order = 5

Figure C.4: Empirical IRFs with Different Number of Lags